TECHNISCHE UNIVERSITÄT MÜNCHEN

Pankreas-Forschungslabor/Chirurgische Klinik und Poliklinik

Klinikum rechts der Isar

In vivo functional dissection of a context-dependent role for Hif1α in pancreatic tumorigenesis

Tao Cheng

Vollständiger Abdruck der von der Fakultät für Medizin der Technischen Universität München zur Erlangung des akademischen Grades eines Doktors der Medizin genehmigten Dissertation.

Vorsitzender: Prof. Dr. E. J. Rummeny

Prüfer der Dissertation:

1. Prof. Dr. J. H. Kleeff (schriftliche Beurteilung)

   apl. Prof. Dr. H. Algül (mündliche Prüfung)

2. Prof. Dr. B. Holzmann

Die Dissertation wurden am 17.11.2016 bei der Technischen Universität München eingereicht und durch die Fakultät für Medizin angenommen.

Table of Contents

ABSTRACT

Hypoxia-inducible factor 1α (Hif1α) is an essential master regulator in mediating cellular response and promoting survival in hypoxia. Genetic ablation of Hif1α has been reported to promote pancreatic ductal adenocarcinoma (PDAC) carcinogenesis by mediating tumour associated inflammation in mice, which questions its role in tumorigenesis of PDAC. We hypothesised that the role of Hif1α in regulating pancreatic tumorigenesis might be context-dependent. To further validate this, we generated murine PDAC cells with Hif1α specific shRNA to downregulate Hif1α expression. Primary tumour growth and metastasis capacity were considered as two main biological scenarios, which were evaluated in vivo through orthotopic transplantation and portal vein injection mouse models. Despite the protective role of stress associated cells deaths, Hif1α depletion resulted in diverse oncogenic consequences. On one hand, Hif1α depletion facilitates tumour growth by triggering hypoxia-induced cell death, which further leads to a persistent tumour-supportive inflammatory response. On the other, the absence of Hif1α reduces hepatic metastasis and impairs metastatic colonisation by inducing anchorage-independent associated cell death. In summary, there is a context-dependent role of Hif1α in PDAC carcinogenesis, which argues for the cautions application of Hif1α inhibitors in clinical management.

1.0 INTRODUCTION

Oxygen is the most important factor in preserving function and survival of cells. In cellular respiration, oxygen serves as the oxidising agent, with which the energy transmitter is generated, and nutrients are converted into smaller molecular for further application [1]. Due to the uncontrolled proliferation of tumour cells, oxygen perfusion is barely enough for tumour proliferation, thus making hypoxia a frequent phenomenon in the majority of solid tumours [2].

1.1 Hypoxia

Hypoxia is a term referring to insufficient oxygen in tissue or ambient air. Normal healthy mammalian tissues preserve around 2%-9% oxygen, when tissue oxygen is lower than 2%, hypoxia occurs; if the oxygen level deteriorates to less than 0.02%, anoxia occurs [3].

There is an interactional play between tumour and hypoxia. On one hand, low oxygen result in inflammation [4], necrosis, aberrant vascularization and metabolic reprogramming in tumour [5]; on the other, outgrow of tumour mass elicits hypoxia, which further facilitates survival and metastasis of tumour cells [6]. Hypoxia has already been recognised as an important hallmark of cancer [7].

1.2 Hypoxia-inducible factors

The master regulator in response to hypoxia environment is hypoxia-inducible factors (HIFs). HIFs are heterodimer protein constituted by an α and β subunit,

among which the most vital one is Hif1α. Under normoxic conditions, Hif1α is expressed in the cytoplasm and degraded by proteasome instantly after synthesis. When under hypoxic conditions, Hif1α protein stabilises due to deactivation of hydroxylation, translocates into nuclear and binds to promoter region in cell nuclear and regulates expression or silence of the target genes [8]. Hence, Hif1α is a master transcription factor for sensing oxygen level in cell and microenvironment. The downstream target genes of Hif1α are reported over 40 in total, whose primary regulation functions are regulating angiogenesis, metabolism, immunity, cell survival and metastasis [9].

1.2.1 Hif1α in angiogenesis

Angiogenesis is a natural process through which neo-vascular is formed from the anterior blood vessel. It is extremely important for tissue growth, development and repair [10].The regulation of Hif1α in angiogenesis can be concluded in: (1) upregulating angiogenic genes such as vascular endothelial growth factor isoforms (VEGFs) and angiopoietin 2 (ANG-2); (2) upregulating proangiogenic factors expression; (3) regulating proliferation and cell cycle of endothelial cells in blood vessel [11]. Therefore, Hif1α is tightly involved in the entire process of angiogenesis.

In tumour tissue, aberrant angiogenesis is recognised as a malignant transformation from benign lesions to disrupted cancerous lesions, in which Hif1α plays an instrumental role [12]. Architectural distortion and futile vessels inside the tumour create persistent hypoxia, activating Hif1α expression continuously. Meanwhile, the genome alteration due to malignant

transformation enhances and stabilises Hif1α protein activity, leading to Hif1α accumulation and upregulating expression of angiogenic genes and proangiogenic factors. However, the neovascularization under pathological conditions is unstable and leaky, which couldn't relieve tumour tissue from hypoxia effectively. This situation may result in a repeated hypoxia and angiogenesis circulation [13]. The periodic cycle is favourable for survival and evasion of metastatic tumour cells from the original organ, thus severe hypoxia or active angiogenesis results in cancer metastasis [14].

1.2.2 Hif1α in anoikis resistance

The extracellular matrix (ECM) provides support for maintaining cell interaction and biological behaviour [15]. The communication between cell to cell, or cell to ECM is essential for sustaining survival and proliferation of adherent cells. When cells lose the connection to other cells or detach from the ECM, anoikis is launched to eliminate the abnormal cells and protect tissue from false re-adhesion of the detached cells in wrong organs [16]. Therefore, anoikis is considered as another type of programmed cell death to defend disordered cell behaviour. Nonetheless, the metastatic tumour cells find solutions to acquire anoikis resistance under suspension situation by regulating essential molecular pathways to avoid from death [17]. Hif1α is confirmed to involve in anoikis resistance regulation.

In order to detach from ECM or cell-cell interaction, cancer cells need to transit cell character from epithelial to mesenchymal, thus most cancer cells escape from anoikis by undergoing epithelial to mesenchymal transition (EMT) [18].

HIF1 contributes to anoikis resistance by upregulating translational factors Snail and Twist, attenuating E-cadherin expression and promoting cell transition from epithelial to mesenchymal phenotype [19]. Moreover, the reactive oxygen species (ROS) accumulation under hypoxia conditions stabilises Hif1α proteins and accelerates EMT process in anchorage-independent cells [20].

Another mechanism of anoikis resistance in cancer cells is the activation of anti-apoptosis or survival signalling. There has been publication reported that Hif1α contributes to anoikis cell survival by exploiting epidermal growth factor receptor (EGFR) and mitogen-activated protein kinases (MAPK) signalling to impair apoptosis-related proteins' accumulation in detached tumour cells [21]. Besides, Hif1α regulates autophagy associated gene expressions to prolong survival and facilitate adaptations to metabolism alteration under anoikis situation [22].

1.2.3 Hif1α in metabolic reprogramming

Tumour cell acquires macromolecular to generate the framework of cytoskeleton from catabolism and anabolism. Due to extensive hypoxia inside tumour tissue, energy supply and demand is imbalanced. Hif1α reprograms adaptive metabolism in tumour cells to maintain homoeostasis and maintain the requirement of tumour proliferation and expansion [23].

Oxidative phosphorylation needs oxygen as an oxidative agent and an electron receptor to generate adenosine triphosphate (ATP). Though it is highly efficient on energy production, moreover, it is not sufficient to produce

substrates for building cytoskeleton of the newly proliferated cells under stressed environment, such as hypoxia. Thus the hypoxic tumour cells switch to glycolysis by activating Hif1α expression.

It has been proved that hypoxic embryonic fibroblasts upregulate expression of pyruvate dehydrogenase (PDH) and lactate dehydrogenase A (LDHA) by coordinating with Hif1α, resulting in higher glycolysis rate and lactate production [24]. Furthermore, Hif1α activates pyruvate kinase M2 (PKM2) expression in tumour cells. The functional PKM2 protein catalyses phosphoenol-pyruvate to pyruvate, which is further converted into lactate. Moreover, PKM2 interacts with Hif1α to enhance the translational effect of Hif1α proteins in regulating metabolic related genes [25].

1.2.4 Hypoxia, pancreatic adenocarcinoma (PDAC) and immune response

The immune system is a physical barrier, protecting human beings against from various kinds of foreign pathogens. According to pathogen types, the response time, immunological memory and responsible immune cells, the immune response can be classified briefly into two typical types: innate immune response and adaptive immune response [26]. Neutrophils, macrophages, natural killer cells, dendritic cells and other mast cells are major innate immunity cells, while T cells and B cells constitute major compartments of the adaptive immunity [27, 28]. In the case of cancer, the immune response is more complicated than general infection or tissue damage.

Fast proliferating neoplastic cells can be recognized as pathogens and eliminated by immunological surveillance at very early stage. However, with the initiation and development of cancerous cells, tumour associated inflammation promotes immune cells recruitment, which plays important roles in promoting tumour growth, genomic instability, angiogenesis and metastasis [29]. Therefore, immunotherapy becomes hot topics on cancer treatments since two decades ago.

There are two prominent features of PDAC. One is high levels of hypoxia in the tumour core, the other is remarkable immune dysfunction [30]. It has been widely accepted that hypoxia is closely correlated with inflammation [31]. Hypo-perfusion and dense fibrous stroma lead to hypoxia, while hypoxic condition contributes to immune dysfunction [32]. As a master sensor and regulator of hypoxia, Hif1α is crucial for regulating intra-tumoral immune response and tailoring microenvironment in PDAC [24, 33].

A recently published paper reported that Hif1α is crucial for recruitment of monocytes/macrophages in PDAC [34]. By analysing PDAC patients' tissue slides, they found positive correlation with Hif1α expression and macrophages infiltration. Subsequent analysis revealed that up-regulation of Hif1α promoted pancreatic stellate cells to secret chemokines 2 (CCL2), which further facilitated monocytes/macrophages recruitment and promoted immune response.

Another research group reported that absence of Hif1α promoted precancerous lesion - pancreatic intraepithelial neoplasia (PanIN) – progression in a pancreas specific Hif1α knock-out mice model [35]. The

derived tumour was accompanied apparently with elevated B lymphocytes infiltration. Deletion of B lymphocytes reversed tumour progress. These results demonstrate that Hif1α plays vital roles in mediating immune response and tumorigenesis.

1.3 Inhibitors targeting hypoxia

Due to the hypoxic character of tumour cells, researchers have been dedicated to developing inhibitors or drugs targeting hypoxia to treat cancer individually. The early attempts focus on the downstream signals of hypoxia, such as angiogenesis. However, the clinical outcome is not as satisfying as expected, and the problem of chemo-resistance urges scientist to develop new generation inhibitors. Nowadays, there are two promising inhibitors targeting hypoxia tested in pre-clinical and clinical trials.

One of them is TH-302, which is activated and release cytotoxic effectors specifically under hypoxia conditions [36]. Preclinical studies showed TH-302 decreases blood flow and inhibit tumour growth of PDAC [36]. Meanwhile, TH-302 in combination with gemcitabine, exhibits encouraging results in advanced and metastatic PDAC patients with prolonged progression-free time and higher tumour response rate [37].

Another promising inhibitor is PX-478, which targets and inhibits Hif1α specifically [38]. Recent data demonstrate that PX-478 in combination with gemcitabine synergistically suppresses tumour growth [39]. Another pre-clinical study tested the effect of PX-478 together with arsenic trioxide in vitro and in vivo [40]. The results showed that PX-478 enhance the effect of

ROS production induced by arsenic trioxide, resulting in apoptosis in PDAC cells. Recently, a phase I trial reported that PX-478 is well tolerated, displaying an anti-tumour activity in advanced stage [41].

2.0 AIMS OF THIS STUDY

PDAC is a cancer entity with remarkable tissue hypoxia [42, 43]. As a master sensor and regulator of hypoxia, Hif1α plays important role in regulating adaptive changes of tumour cells in response to cellular stress and promoting cell survival under hypoxia conditions [44]. Clinical data revealed that high expression of Hif1α was correlated with poor prognostics and overall survival in PDAC patients [45]. Hif1α can be stabilized under normoxia conditions by hyper-activated mechanistic target of rapamycin (mTOR) signalling [46]. Deletion of Hif1α in a pancreas-specific Kras^{G12D} mutant mouse model promoted PDAC progression with elevated B lymphocyte infiltration [35]. These evidences argue for a context-dependent role of Hif1α in pancreatic tumorigenesis. Therefore, it is pivotal to investigate the role of Hif1α in PDAC.

We have already generated and isolated a murine PDAC cell line 399 (p48^{Cre};LSL-Kras^{G12D};Tsc1$^{fl/+}$), which is hyper hypoxic.

Based on the data and mouse model in existence, we would ask following questions:

(1) What is the effect of Hif1α deletion on murine PDAC cells?

(2) What is the in vivo function of Hif1α?

(3): Is it practical to apply HIF1α inhibitor in clinical management?

3.0 MATERIALS AND METHODS

3.1 Materials

3.1.1 List of antibodies

Primary antibodies

Antibody name	Catalogue number	Application* (Reactivity**)	Producer
Mouse Anti-B220/CD45R Ab[#]	MAB1217	IHC (M)	R&D Systems (Wiesbaden, Germany)
Rabbit Anti-CD3 (SP7) Ab[#]	ab16669	IHC (M)	Abcam (Cambridge, UK)
Rat Anti-mouse CD45 (Clone 30-F11) Ab[#]	550539	IHC (M)	BD Biosciences (Heidelberg, Germany)
Rabbit Anti-Cleaved Casp3 mAb[#]	9664	WB; IHC (M)	Cell Signaling Technology (Frankfurt am Main, Germany)
Rat Anti-mouse F4/80 (BM8) Ab[#]	MF48000	IHC (M)	Thermo Fisher Scientific (Dreieich, Germany)
Rabbit Anti-GAPDH Ab[#]	sc-25778	WB (M)	Santa CruzBiotechnology (Heidelberg, Germany)
Moue Anti-Hif1 α Ab[#]	NB100-105	WB (M)	Novus(Abingdon,UK)

Rabbit Anti-Hk2 mAb[#]	2867	WB (M)	Cell Signaling Technology
Rabbit Anti-Glutaminase Ab[#]	Ab156876	WB (M)	Abcam
Rabbit Anti-Myeloperoxidase Ab[#]	CMC28917023	IHC (M)	Cell Marque (Rocklin, CA, USA)
Mouse Anti-β actin Ab[#]	sc-69879	WB (M)	Santa Cruz Biotechnology
Rabbit Anti-p-Histone H3 (Ser10) Ab[#]	9701	IHC (M)	Cell Signaling Technology

Secondary antibodies

Antibody name	Catalog number	Application*	Producer
Rabbit HRP (horseradish peroxidase)- labelled Anti-Rat IgG Ab[#]	P0450	IHC (M)	Dako Deutschland GmbH (Hamburg, Germany)
Goat HRP-Labelled Polymer Anti-Mouse Ab[#]	K4001	IHC (M)	Dako Deutschland GmbH
Goat HRP-Labelled Polymer Anti-Rabbit Ab[#]	K4003	IHC (M)	Dako Deutschland GmbH
Sheep HRP-labelled Anti-Mouse IgG Ab[#]	NA931	WB (M)	GE Healthcare (Little Chalfont, UK)
Donkey HRP-labelled Anti-Rabbit IgG Ab[#]	NA934	WB (M)	GE Healthcare

*Application key: WB = western-blot; IHC = Immunohistochemistry; **Reactivity key: M = mouse; #Ab: antibody

3.1.2 Chemicals and Reagents

0.25% trypsin/EDTA	Sigma-Aldrich Chemie GmbH (Munich, Germany)
2-Deoxy-D-glucose	Sigma-Aldrich Chemie GmbH
2-Deoxy-D-glucose 6-phophate sodium salt	Santa Cruz Biotechnology
2-Mercaptoethanol	Sigma-Aldrich Chemie GmbH
β-Nicotinamide adenine dinucleotide phosphate sodium salt hydrate	Sigma-Aldrich Chemie GmbH
Acetic acid	Merck Biosciences (Darmstadt, Germany)
Acetic anhydride	Sigma-Aldrich Chemie GmbH
Acrylamide solution	Carl Roth (Karlsruhe, Germany)
Agarose	Carl Roth
Albumin Fraction V (BSA)	Carl Roth
Ammonium persulfate (APS)	Sigma-Aldrich Chemie GmbH
Biocoatmatrigel invasion unit	BD Biosciences (Franklin Lakes, NJ, USA)

Calcium chloride	Carl Roth
Cell lysis buffer (10x)	Cell Signaling Technology
Chloroform	Merck Biosciences
Citric acid monohydrate	Carl Roth
Crystal violet	Carl Roth
Dimethyl sulfoxide	Carl Roth
Diaphorase from Clostridium kluyveri	Sigma-Aldrich Chemie GmbH
Dulbecco's MEM	Sigma-Aldrich Chemie GmbH
ECL detection reagent	Amersham (Little Chalfont, UK)
Ethanol	Carl Roth
Ethidium bromide	Carl Roth
Ethylenediaminetetraacetic acid disodium salt dihydrate	Carl Roth
Foetal bovine serum	Sigma-Aldrich Chemie GmbH
Formamide	Merck Biosciences
Glucose-6-phosphate Dehydrogenase	Sigma-Aldrich Chemie GmbH
Glycerol	Merck Biosciences

Glycine	, Diagnostics (Penzberg, Germany)
Haematoxylin	Merck Biosciences
HEPES	Carl Roth
Hydrochloric acid (5M)	Apotheke TU München (Munich, Germany)
Hydrogen peroxide (30%)	Carl Roth
Histowax	Leica (Wetzlar, Germany)
Isopropanol	Carl Roth
Kaliumchlorid (potassium chloride)	Carl Roth
LDS sample buffer (4x)	Thermo Fischer Scientific
L-Glutamine	Sigma-Aldrich Chemie GmbH
Liquid nitrogen	Tec-Lab (Taunusstein, Germany)
Liquid DAB & chromogen substrate	DakoCytomation
Magnesium Sulfate	Sigma-Aldrich Chemie GmbH
Methanol	Merck Biosciences
Molecular weight marker	FERMENTAS/Termo (Dreieich, Germany)
MOPS	Carl Roth
Dinatriumhydrogenphosphate	Merck Biosciences

Nitrocellulose membranes	GE Healthcare
Normal goat serum	DakoCytomation
Nuclear and cytoplasmic extraction reagents	Thermo Fischer Scientific
Para-formaldehyde	Apotheke TU München
Phosphate buffered saline (PBS) pH 7.4	Sigma-Aldrich Chemie GmbH
Polyvinylpyrrolidone	Sigma-Aldrich Chemie GmbH
Permount	Vector Laboratories (Burlingame, CA, USA)
Penicillin-Streptomycin	Sigma-Aldrich Chemie GmbH
Phosphatase inhibitor cocktail	Roche diagnostics
Protease inhibitor cocktail	Roche diagnostics
Proteinase K	DakoCytomation
Resazurin sodium salt	Sigma-Aldrich Chemie GmbH
RNAseDNAse-free water	Invitrogen (Karlsruhe, Germany)
Rotiphorese Gel 30 (37,5:1)	Carl Roth
Sample reducing buffer (10x)	Thermo Fischer Scientific
SDS ultra pure	Carl Roth

Sodium borate	Merck Biosciences
Sodium chloride	Carl Roth
Sodium citrate	Merck Biosciences
Sodium hydroxide (5M)	Apotheke TU München
Sodium phosphate	Merck Biosciences
TEMED	Carl Roth
Tetraethylammonium chloride	Sigma-Aldrich Chemie GmbH
Thiazolyl Blue Tetrazolium Bromide (MTT)	Sigma-Aldrich Chemie GmbH
Triethanolamine	Sigma-Aldrich Chemie GmbH
Tris base	Sigma-Aldrich Chemie GmbH
Triton X 100	Carl Roth
Trypan blue solution	Sigma-Aldrich Chemie GmbH
Tween 20	Carl Roth
PBS powder without Ca^{2+}, Mg^{2+}	Biochrom AG (Berlin, Germany)

3.1.3 Buffers and Solutions

Immunohistochemistry

10x Tris Buffered Saline (TBS)

Tris base	12.1 g
NaCl	85 g
Distilled Water	800 ml
Adjust pH to 7.4 with	5 M HCl
Constant volume with distilled water to	1000 ml

20x Citrate buffer

Citric acid (Monohydrate)	21.0 g
Distilled water	300 ml
Adjust to pH 6,0 with	5 M NaOH
Constant volume with distilled water to	500 ml

Washing Buffer (1xTBS+0.1%BSA)

10xTBS	100 ml
BSA	1 g
Constant volume with distilled water to	1000 ml

Western Blott

Electrophoresis buffer

MOPS	209.2 g

Tris Base	121.2 g
SDS	20 g
EDTA-free acid	6 g
Constant volume with distilled water	to 1 l

Transfer Buffer

Tris base	29.1 g
Glycine	14.7 g
Methanol	1000 ml
SDS	0.1875 g
Constant volume with distilled water	to 5 l

Washing buffer

10xTBS	100 ml
Tween 20	0.5 ml
Constant volume with distilled water	to 1000 ml

Blocking Buffer

Dry milk or BSA	0.5 g
Washing buffer	10 ml

Glucose uptake

KRH (Krebs-Ringer-HEPES) buffer

HEPES	50 mM
NaCl	137 mM
KCl	4.7 mM
$CaCl_2$	1.85 mM
$MgSO_4$	1.3 mM
BSA	0.1% (w/v)
Adjust to pH 7.4 with	0.5 M NaOH

TEA (triethanolamine) buffer, 200 mM

TEA	200 mM
Adjust to pH 8.1 with	1 M NaOH
Constant volume with distilled water	to 50 ml

Assay solution

200 mM TEA	2.5 ml
0.4% BSA	500 µl
10 mM NADP	100 µl

Diaphorase	2 units
2mMResazurin sodium salt	10 µl
L mesenteriodes G6PDH	150 units
Constant volume with distilled water	to 10 ml

3.1.4 Kits

Mouse VEGF Quantikine ELISA Kit	R&D Systems
Mouse Serum Amyloid A ELISA Kit (SAA)	Abcam
BD Cytometric Bead Array(CBA) Mouse EnhancedSensitivity Master Buffer Kit	BD Biosciences
Mouse IL-6 Enhanced Sensitivity Flex Set	BD Biosciences
Mouse TNF Enhanced Sensitivity Flex Set	BD Biosciences
Extracellular Matrix and Adhesion Molecules RT2 Profiler PCR Array	Qiagen (Hilden, Germany)

3.1.5 Laboratory equipment

Analytic balance	METTLER (Giessen, Germany)

Balance	SCALTEC (Göttingen, Germany)
Biophotometer	Eppendorf (Hamburg, Germany)
Centrifuge	Eppendorf
CO_2 incubator	SANYO (Secausus, NJ, USA)
Computer Hardware	Fujitsu SIEMENS (Tokyo, Japan)
Electrophresis/Electroblotting equipment/ power supply	Invitrogen
Freezer -20°C	LIEBHERR (Bulle, Switzerland)
Freezer -80°C	Heraeus (Hanau, Germany)
Fluorescence reader	Promega
Luminescence reader	Promega
Microplate reader	Thermo Fischer Scientific (Dreieich, Germany)
Microscope	LEICA (Wetzlar, Germany)
Microwave oven	SIEMENS (Munich, Germany)
PH-meter	BECKMAN (Washington, DC, USA)
Power supply	BIOMETRA (Göttingen, Germany)
Refrigerator 4°C	COMFORT (Buller, Switzerland)
Roche LightCycler 480	Roche

Roller mixer	STUART (Stone, UK)
Scanner	Canon (Tokyo, Japan)
Spectrophotometer	Thermo Fischer Scientific (Dreieich, Germany)
Sterilgard Hood	Thermo Fischer Scientific (Dreieich, Germany)
Thermomixer	Eppendorf
Vortex Mixer	NEOLAB (Heidelberg, Germany)
Water bath	LAUDA (Lauda-Koenigshofen, Germany)
Stereomicroscope	Zeiss
Tissue embedding machine	Leica (Wetzlar, Germany)
Tissue processor	Leica
Glucose meter (Precision Xceed)	Abbott GmbH (Wiesbaden, Germany)

3.1.6 Consumables

Blotting paper	Whatman (Maidstone, Kent, UK)
Cell scraper	SARSTEDT (Nuembrecht, Germany)
Coverslips	MENZEL (Braunschweig, Germany)
Filter (0.2 µm)	NEOLAB (Heidelberg, Germany)

Filtertip (10 µl, 20 µl, 100 µl, 200 µl, 1000 µl)	Starlab
Hyperfilm	GE Healthcare (Little Chalfont, UK)
Pure Nitrocellulose membrane (0.45 µM)	BIO-RAD
Sterile needles	BD (Franklin Lakes, NJ, USA)
Tissue culture dishes (60x15 mm; 100x20 mm)	SARSTEDT (Nuembrecht, Germany)
Tissue culture flasks (25 cm^2; 75 cm^2; 125 cm^2)	GREINER
Tissue culture plates (6-well; 24-well; 96-well)	GREINER
Ultra-Low attachmentmultiwell plates (24-well)	Sigma
Ultra-Low attachment cell culture flasks (25 cm^2)	Sigma
Tubes (15 ml; 50 ml)	GREINER

3.2 Methods

3.2.1 Cell culture

399 cell line from p48^{Cre}; LSL-Kras^{G12D}; Tsc1$^{fl/+}$ mouse was cultured with high glucose DMEM medium (Sigma -Aldrich) containing 10% fetal bovine serum (FBS), 100 u/ml of penicillin, and 100 µg/ml of streptomycin at 37ºC, 5% CO_2.

3.2.2 Stable transfection of cell lines

For the generation of stable clones with low expression of Hif1α, 399 cells were transfected with 10 µg of Hif1α shRNA plasmid (Santa Cruz Biotechnology) or control shRNA plasmid (Santa Cruz Biotechnology) in 10 cm dishes. Single clones were picked by selection medium with Puromycin (Santa Cruz Biotechnology). The knock-down was confirmed by immunoblot analysis.

3.2.3 Immunohistochemistry analysis

Tissue was fixed with 4% formaldehyde, embedded in paraffin and cut into 2,5 µm sections. After deparaffinized and rehydrated, the tissue section was performed on antigen retrieval with citrate buffer (pH 6.0; 10 mM citric acid, 0.05% Tween 20) in amicrowave oven for 12-15 minutes or with proteinase K (Dako) for 15 minutes. After endogenous peroxidase and non-specific binding blocking, the sections were incubated with thefirst antibody at 4ºC for overnight. The specific antibody dilution was: anti-cleaved Caspase-3 (CellSignalling Technology) at 1:500; anti-phospho-Histone H3 (Cell Signalling Technology) at 1:500; anti-Myeloperoxidase(Cell Marque) ready-to-use; anti-B220 (R&D Systems) at 1:1000; anti-CD45 (BD Biosciences) at 1:10; anti-F4/80 (Thermo Fisher Scientific) at 1:100; anti-CD3 (Abcam) at 1:100. Following incubation,Liquid DAB+ Substrate Chromogen System (Dako) was used for thecolour reaction. Subsequently, sections were counterstained with

Mayer's hematoxylin, dehydrated with ethanol and roticlear, and mounted with Permount(Vector Laboratories).

3.2.4 IHC positive stained cells quantification

Every slide was taken pictures at five random field of view by a Carl Zeiss microscope under 20x (for pH-H3) or 40x (for all immune cell staining) objective lens. The number of positive stained cells in every picture was calculated by two independent researchers with the ImageJ (1.51f) software.

3.2.5 mRNA and cDNA preparation

The mRNA extraction and cDNA revers-transcription were performedfollowing manufacturer's instructions from mRNA extraction kit (Qiagen) and cDNA transcription kit (Qiagen).

3.2.6 Quantitative Real-Time Chain Reaction

Quantitative real-time PCR (QRT-PCR) was performed to examine theexpression level of Hif1α and housekeeping gene PpiB (Peptidylprolyl Isomerase B) with SYBR Green I Master kit (Roche Diagnostics). The primer sequences were as presented as follows: Hif1α, 5'-ACCTTCATCGGAAACTCCAAAG-3' and 5'-CTGTTAGGCTGGGAAAAGTTAGG-3'; PpiB, 5'-GGAGCGCAATATGAAGGTGC-3' and 5'-

CTTATCGTTGGCCACGGAGG-3'. Relative gene expression was analyzed with LightCycler[TM]480 software (Roche Diagnostics).

3.2.7 Immunoblot analysis

Protein extraction from cells

Total protein was extracted by using cell lysis buffer (Cell SignallingTechnology) containing protease inhibitor (Roche) and phosphatase inhibitor (Roche). Nuclear and cytoplasmic protein were prepared using NE-PER™ Nuclear and Cytoplasmic Extraction Reagents(ThermoFisher Scientific). Protein concentration was determined by BCA protein assay kit (ThermoFisher Scientific).

Western blotting

20µg proteinswere electrophoretically separated in 10% SDS-PAGE, andelectro-transferred to PVDF membranes. After blocked with 5% milk or 5%, the membrane was incubated with first antibodies at 4 ºC overnight. Following first antibody incubation, the membrane was washed and incubated with Horseradish peroxidase (HRP)-conjugated secondary antibody at room temperature for 1 hour. Afterwards, target band signals were detected withAmersham ECL Western Blotting Detection Reagent (GE Healthcare Life Sciences).

Western blotting quantification

The films with detectable band signals are scanned with CanoScan 4400F (Canon Deutschland) at high resolution pictures (Tiff format). The protein

densitometry on film pictures is measured with ImageJ (1.51f) according to instructions from University of Queensland Diamantina Institute (http://www.di.uq.edu.au/sparqimagejblots)

3.2.8 Mouse Vegfa Elisa measurement

Vegfa secretion in theFBS-free medium was measured with VEGF quantikine ELISA Kit (R&D Systems).Same amounts of cells were seeded in 6-well plates. The cells were incubated with 1 ml FBS-free culture medium for 24 hours. Subsequently,the supernatant was collected in control cells and Hif1α knock-down cells. Vegfa concentration in each cell linewas determined following the instruction book inside the kit.

3.2.9 Mouse serum amyloid A (SAA) Elisa measurement

SAAconcentration in the mouse serumwas derterminedaccording to instruction's book fromthe mouse serum amyloid A ELISA kit (SAA) (Abcam).Generally, the mouse serum samples from control and Hif1α knock-down groups were diluted at 1:1000 with 1x dilute provided in the kit. After sample application, HRP conjugated antibody incubation and colour development, the SAA concentration of every serum sample was calculated according to standard curves.

3.2.10 Il6 and TNFα measurement

The concentrations of Il6 and TNFα in mouse serum were determined by bead-based immunoassays. Generally, the mouse serum in control and Hif1α knock-down group was diluted at 1:5 with assay dilute provided in the BD cytometric bead array(CBA) mouse enhanced sensitivity master buffer kit (BD Biosciences). After incubation with Il6 or TNFα capture beads (BD Biosciences) and detection reagent, the signals of serum samples and standard samples were detected on a flow cytometer. The data was analyzedwith FCAP Array software (v3.0) according to the user's guide..

3.2.11 Colony formation assays

$3 \times 10^2$of logarithmic phase cells were counted and seeded in 6 -well plate.Afterwards, the cells were cultured at normal condition continuously for 7 days. Maintain the culture medium unchanged during the whole cultivation.At end point, Culture medium was removed, 100% methanolwas used for colony fixation, and 10% crystal violetwas applied for staining. The number of formed colonies containing more than 50 cells was counted by two researchers respectively.

3.2.12 MTT assay

2000 cells in100μlmediumwere seededin 96 well plates. At specific time point, 50μg Thiazolyl Blue Tetrazolium Bromide (MTT, Sigma-Aldrich) was applied to cells and incubated at culture conditions for 4 hours. Then the formed

precipitates were dissolved in 100µl 2-propanol. Cell proliferation was determined by measuring absorbance values under 570nm.

3.2.13 Invasion assay

Invasion assay was performed by employing transwell chamber system from Thermo Fischer Scientific. Control or Hif1α knock-down cells were counted and re-suspended with theFBS-freemedium. The upper chamberwas addedto 200 µl cell suspension containing 2×10^4 cells. Meanwhile, the lower chamber was added with 500µl culture medium containing10%FBS.After 24 hours incubation, the chamber membrane was fixed and stained following the manufacturer' instruction.The invaded cell number in each group was counted by two independent researchers separately.

3.2.14 Cell transplantation experiment

8 weeks old C57BL/6J mice were performedfor tumour cell transplantation. For orthotopicxenograft model, Hif1α knock-down cell or control cell (1×10^6) was transplanted into the mouse pancreas. The operated mice were kept for4 weeks before sacrificed. Pancreatic tumour and mouse serum were collected. For hepatic metastasis model, 5×10^5 of Hif1α knock-down or control cells were injected intothe portal vein. After 2 weeks, operated mice were sacrificed, and the whole liver (left lobe, median lobe, right lobe and caudate lobe)was collected. All studies were performed under the agreement of a protocol approved by the Animal Care and Use Committee of Technical University of Munich (ethical application approval no.1180-14).

3.2.15 Glucose uptake assay

Glucose uptake was measuredaccording to instructions published by Yamamoto's group [47].Briefly, Hif1αcell or control cellwas counted and seeded in a 24-well plate, 2mM 2-DG (Sigma Aldrich) was applied to cells for 20 minutes. Then intracellular DG6P concentration was determined by fluorescence signals at λex=530-570nm λem=590-620nm.

3.2.16 Glutamate assay

Intracellular glutamate lever was measured by using Glutamate assay kit (Abcam). A10^6 cell pellet was re-suspended in 100 μl assay buffer and centrifuged at 13,000×g for 10 minutes. The un-dissolvable material was discarded, the supernatant was collected andtransferred into a 96-well plate. After colour reaction with, the intracellular glutamate level was determined by measuring optical density at 450 nm.

3.2.17 Lactate secretion assay

10^4 cells from each group were seeded in the 96 well plate with culture medium. After 24 hours, the medium was collected, and lactate secretion assay was performed at clinical chemistry department of Klinikum Rechts derIsar (TUM, Munich,Germany)

3.2.18 Anoikis assay

500 µl cell suspension containing $5×10^4$ cells was seeded in an anchorage resistant plate (07-200-602, Sigma-Aldrich,). Cells were cultured under standard conditions for 24 hours before added with 50 µL of 250 µg MTT (M5655, Sigma-Aldrich). Afterwards, cells were incubated for 4 hours at 37 ºC, and added with 500 µL of cell lysis buffer (10% SDS, 0.01 M HCl), and kept culturing in the dark for 24 hours. After incubation 200 µL mixture was transferred into a 96-well plate and absorbance value was measuredat 570 nm.

3.2.19 ECM and adhesion molecular array analysis

The mouse extracellular matrix (ECM) and adhesion molecular array analysis were performed according to the instruction book in a commercial extracellular matrix and adhesion molecules RT^2 Profiler PCR Array kit (Qiagen). The differentiated gene expression were analysed according to the web-based software (www.sabiosciences.com/pcr/arrayanalysis.php).

3.2.20 Liver metastasis area ratio analysis

Hematoxylin and eosin staining was performed on tissue sections to determine histological features. Afterwards, every slidewas scanned with a1.25× object by using Zeiss microscope. The total metastatic burdens weredeterminedas a ratio of thecross-sectional area occupied by thetumour to thewhole liver area using ImageJ(NIH) and Matlab (R2015a).

3.2.21 Statistical analysis

The GraphPad Prism 6 Software (GraphPad) was used for statistical analysis. The data was a result of theindependent triplicate experiment. An unpaired Student's *t*-test was used for determining statistical significance, where $p<0.05$. All values are presentedas mean ± standard error of the mean (SEM).

4.0 RESULTS

Previously, we characterised murine PDAC tumour cell line 399 derived from p48^{Cre};LSL-Kras^{G12D};Tsc1$^{fl/+}$, which was sensitive to hypoxia induction [42, 48]. Therefore this cell line was chosen for our study.

To investigate the role of Hif1α in murine PDAC cells, we stably transfected murine PDAC cell line 399 with the scramble (shCon) and Hif1α knock-down (shHif1α) plasmids. Western blot result confirmed an approximate 90% reduction of Hif1α protein expression after 24 hours' hypoxia exposure (Figure 1a, $p<0.0001$). Meanwhile, the QRT-PCR experiment validated a 60-70% reduction of Hif1α mRNA expression under both normaxia (20% O_2, Figure 1b, $p=0.0001$) and hypoxia (1% O_2, Figure 1b, $p=0.0002$) conditions. These results indicated that Hif1α was significantly down-regulated in the shHif1α group (Figure 1).
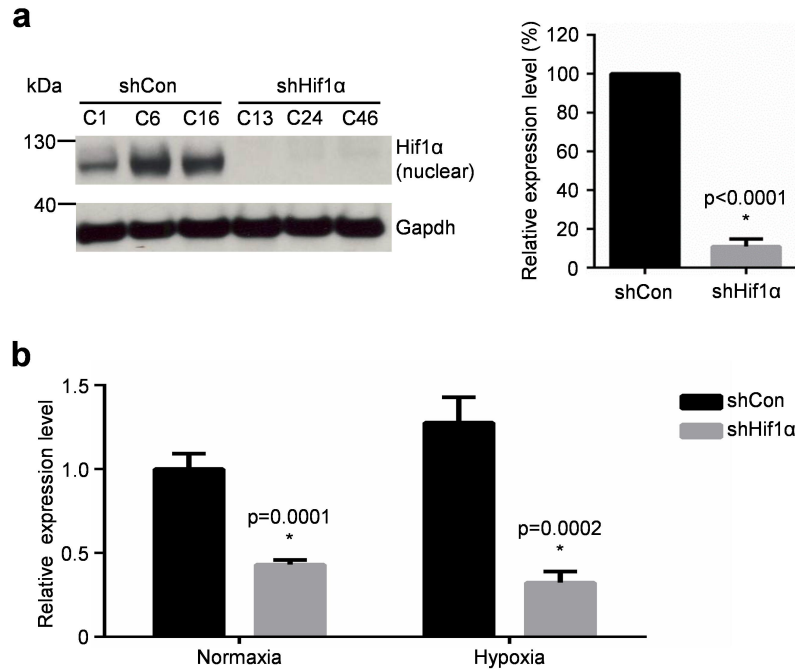
Figure 1. (a) The western blot and quantification result shows a significant reduction of Hif1α expression in shHif1α group; Thesis data has already been published in **(b)** QRT-PCR results confirm the l knock-down of Hif1α in 399 cell line; The data was presented as mean±SEM from triplicate independent experiments; shCon: scramble control plasmid; shHif1α: Hif1αknock-down plasmid. (a-b) has been already published in [49].

Since Hif1α plays a major role in pancreatic cancer metabolism, we compared nutrient intake between shCon cells and shHif1αcells. Consistent with previous data, Hif1α depletion led to significant reductions in glucose uptake (Figure 2a, 17.5±2.54 vs 34.7±2.80 nmol/10000 cells, p=0.0005), intercellular glutamate (Figure 2b, 1.1±0.29 vs 2.7±0.61 nmol, p=0.0481) and lactate secretion (Figure 2c, 1.5±0.14 vs 2.3±0.17 ng/ml, p=0.0049). Along with the metabolic inhibition, there was a compensative upregulation of hexokinase-2 (Hk2) and glutaminase (Gls) protein expression in the shHif1α group (Figure 2d). Protein densitometry analysis revealed that there was an 8.5 folds upregulation of Hk2

in the shHif1α cells (Figure 2d, middle panel, p=0.0001), which demonstrated more pronounced effects of Hif1α on glucose rather than glutamine metabolism.
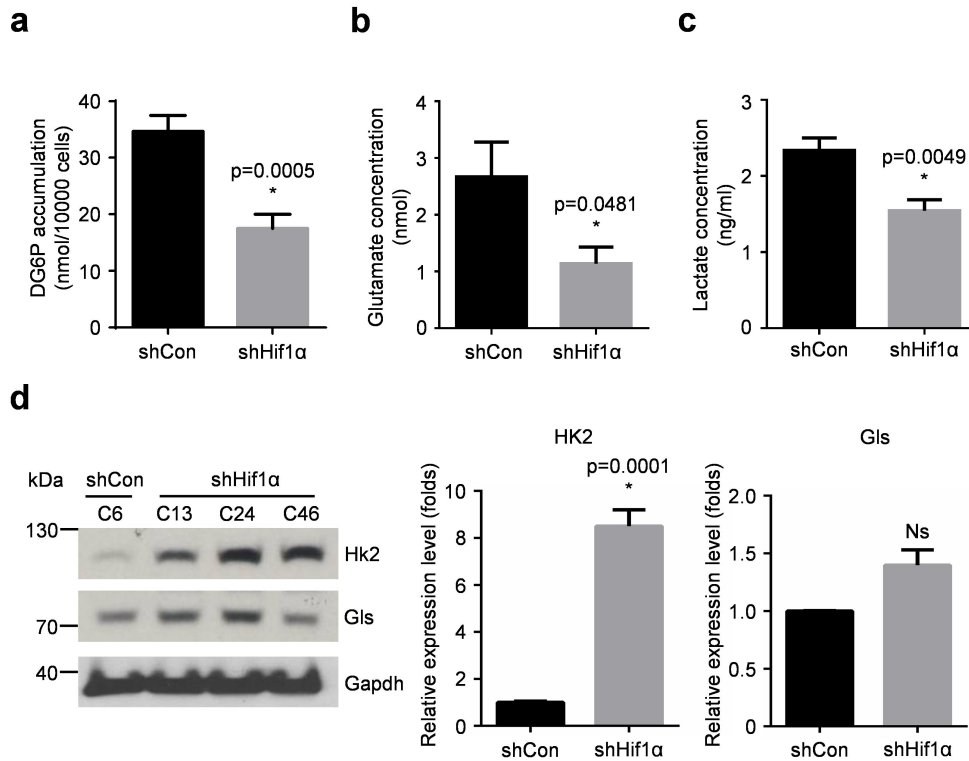
Figure 2. (a) Glucose uptake assay shows a decreased glucose intake in Hif1α deletion group; **(b)** Glutamate assay reveals impaired intracellular glutamate level when Hif1α is absent in 399 cells; **(c)** Lactate secretion measurement illustrates a diminish lactate production in Hif1α deletion group; **(d)** The western blot and quantification result show compensative upregulations of Hk2 and Gls expression due to deletion of Hif1α; The values are presented with means±SEM from three independent experiments; *p* values are determined by an unpaired *t*-test. (a-c) has been already published in [49].

Evidence points out that Hif1α is crucial in regulating physiological and pathophysiological cellular proliferation [50]. Thus we performed colony formation (Figure 3a) and MTT assay (Figure 3b) to determine whether Hif1α was essential for PDAC growth. Our result showed that proliferation ability was not affected due to the deletion of Hif1α.
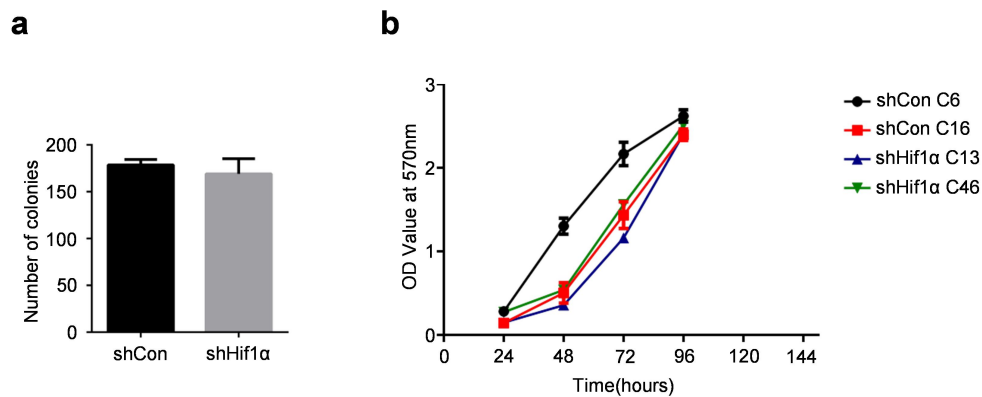
Figure 3. The colony formation **(a)** and MTT proliferation assay **(b)** shows proliferation ability is not affected by knocking down of Hif1α expression. The data are presented as mean±SEM from three independent experiments. (a) has been already published in [49].

However, the invasion capacity was remarkably reduced in the shHif1α cells under both normoxic (20%O_2, p=0.005) and hypoxic (1%O_2, p<0.0001) conditions (Figure 4a). Meanwhile, the different response of control cell and Hif1α deficient cell under hypoxic conditions suggested that hypoxia probably promoted invasion in an Hif1α-dependent manner (Figure 4a).

As vascular endothelial growth factors A (Vegfa) is directly regulated by Hif1α in angiogenic process [51], next we measured the secretion of Vegfa between control and Hif1α knock-down cells. As expected, the Hif1α extinction led to

about 67% reduction of Vegfa secretion in the culture medium (Figure 4b, 248.2±68.66 vs 758.7±68.66 pg/ml, p=0.0046).
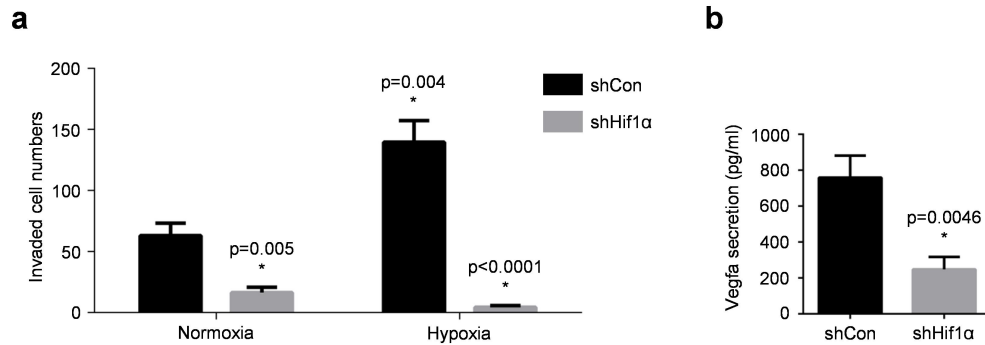

Figure 4. (a) Hif1α deficient cells shows reduced invasion capacity under both normoxic and hypoxic conditions; **(b)** Hif1α deficient cell secretes less Vegfa than control cell. The data are a result of three independent experiments; The value is presented as mean±SEM and *p* value is determined by unpaired *t*-test. (b) has been already published in [49].

In summary, the absence of Hif1α in murine PDAC cells resulted in impaired glucose uptake, reduced intracellular glutamate level, and lactate secretion. Though proliferation was not affected, invasion capacity and Vegfa secretion were obviously inhibited by Hif1α deletion.

To verify whether the phenotype was consistent with in vitro situations, next we transplanted shCon and shHif1α cells orthotopically into the pancreas of C57BL/6J (wild-type, WT) mice (Figure 5a). Surprisingly, tumour mass from the shHif1α group exhibited with a significant larger volume than the shCon

group (Figure 5b, 1.9±0.38 vs 0.1±0.06 cm^3, p=0.0079), which was contradictory with the previous in vivo result.
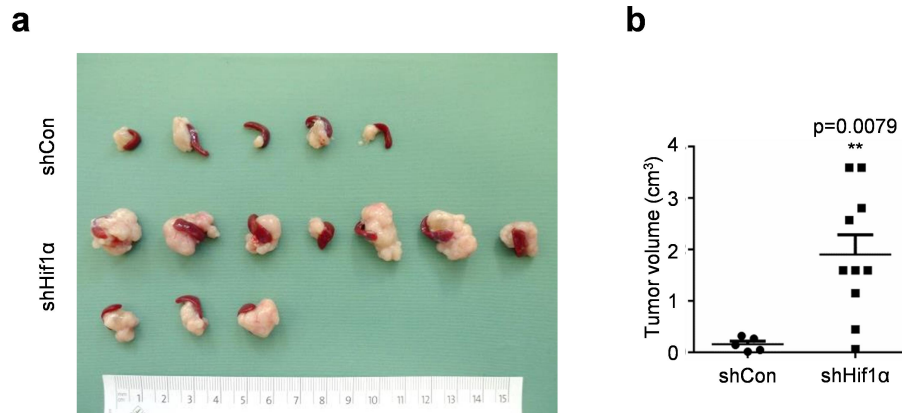
Figure 5. (a) Representative picture of pancreas orthotopic injection model shows a clear shrinkage of tumour volume on Hif1α deletion group; **(b)** Ex vivo volume measurements confirm the synergic role of HIF1 deletion in tumour growth; The data is expressed as mean±SEM and *p* value is determined by unpaired *t*-test. This data has been already published in [49].

Meanwhile, the histological examination indicated that there was obviously larger necrotic area in the shHif1α group (Figure 6a). By employing cleaved-Caspase 3 as a marker to define the boundary of the necrotic region [42], necrotic area measurement was performed between the shCon and shHif1α group. As expected, the necrosis area in the shHif1α group occupied about 22% of the whole tumour area, while that in the shCon group was only 0.7% (Figure 6b, middle panel, p<0.0001). In line, the shHif1α cells were more vulnerable to apoptosis in vitro, especially under hypoxia conditions (Figure 6c, right panel, p=0.0297). Since the non-necrosis area in shHif1α group was still larger than that in the control group (Figure 6b, right panel, 0.7±0.08 vs

0.3±0.97 cm^2, p=0.0261), we hypothesized that the outgrowth of shHif1α derived tumours was due to increased proliferation capacity.
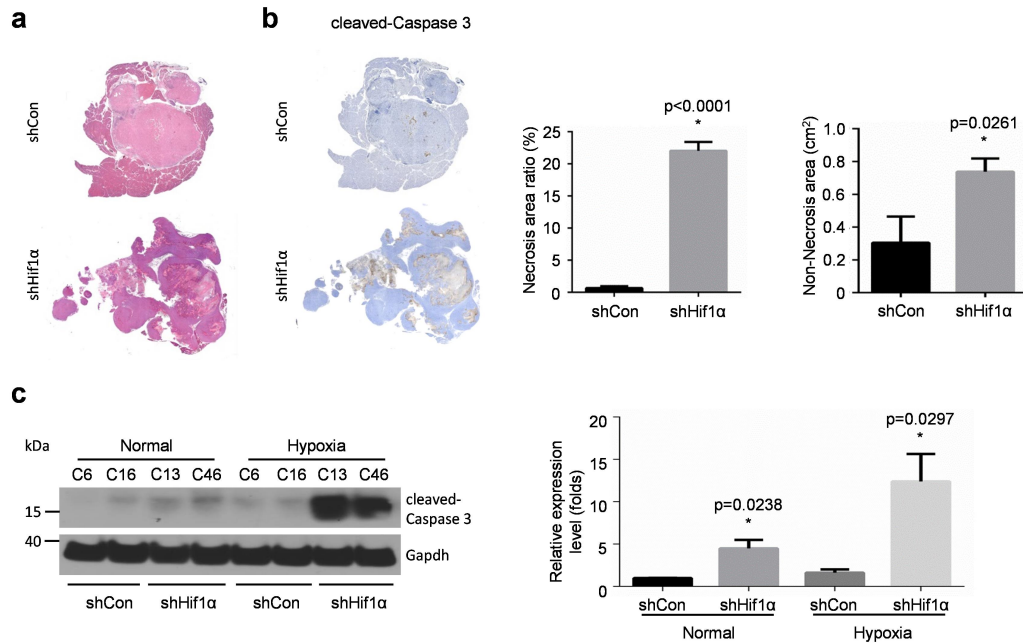
Figure 6. (a) Representative pictures of H&E staining show a prominent necrosis phenotype in Hif1α knock-down group (n=5); **(b)** Representative pictures of cleaved-Caspase 3 staining (left panel) and positive cells quantification (middle panel) demonstrate larger necrosis area in Hif1α knock-down group (n=5); Non-necrosis area quantification shows a larger solid region in the Hif1α knock-down group (right panel); **(c)** Western blot (left panel) and quantification analysis (right panel) result show elevated expression of cleaved-Caspase 3 in Hif1α deletion group under hypoxic conditions; The data is expressed as mean±SEM and *p* value is determined by unpaired *t*-test. This data has been already published in [49].

Indeed, there were more positive stained cells of phospho-histone H3 in the solid tumour area of shHif1α group (Figure 7a), which indicated a significant

increase of proliferation in the shHif1α cell derived tumours (Figure 7b, p=0.0006).
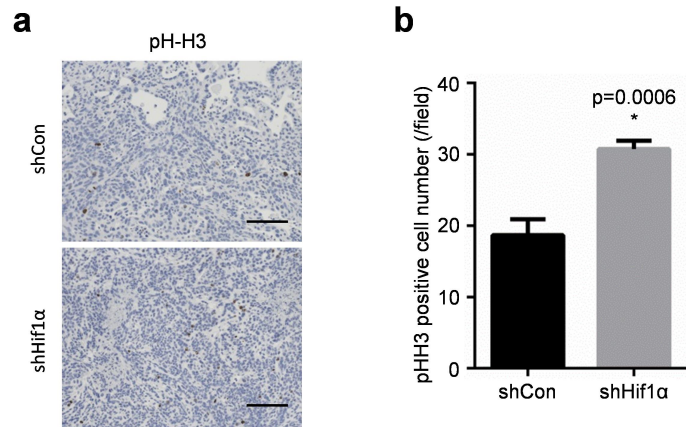
Figure 7. (a) Representative pictures of pH-H3 staining show increased positive cells in Hif1α knock-down group; **(b)** Counting result of positive stained cells confirms active proliferation ability in the shHif1α group; The data are presented as mean±SEM and *p* value is determined by unpaired *t*-test, n=5. This data has been already published in [49].

Tumour growth is a consequence of the interplay between the tumour cell and microenvironment. The compartment of microenvironment plays a major role in regulating cell proliferation. It has been recognised that necrotic cells release death signals and stimulate inflammation [52]. Meanwhile, tumour associated inflammation affects cell proliferation [53]. Based on the existing knowledge, we hypothesised that the development of shHif1α tumours resulted in pronounced necrosis in the tumour mass, which triggered elevated inflammatory response. Immune cell infiltration might be the reason for uncontrolled growth of the shHif1α tumours.

In order to define inflammatory response between the shCon group and the shHif1α group, first we measured concentrations of several inflammatory markers in the mouse serum between two groups. To note, the concentrations of three tested markers - serum amyloid A (SAA), Il6 (interleukin 6) and TNFα (tumour necrosis factor α) – in shHif1α group were increased from different extent. The SAA concentration in shHif1α group was 262.0±12.0 μg/ml, while that in the shCon group was only 199.8±1.92 μg/ml (Figure 8a). Similarly, the Il6 and TNFα concentrations in the shHif1α group were 19.0±4.89 pg/ml and 19.0±2.84 pg/ml respectively, while those in the shCon group were only 5.1±0.94 pg/ml and 8.7±1.20 pg/ml (Figure 8b-c). To conclude, these data proved that the immune response in the shHif1α group was more severe than the shCon group.
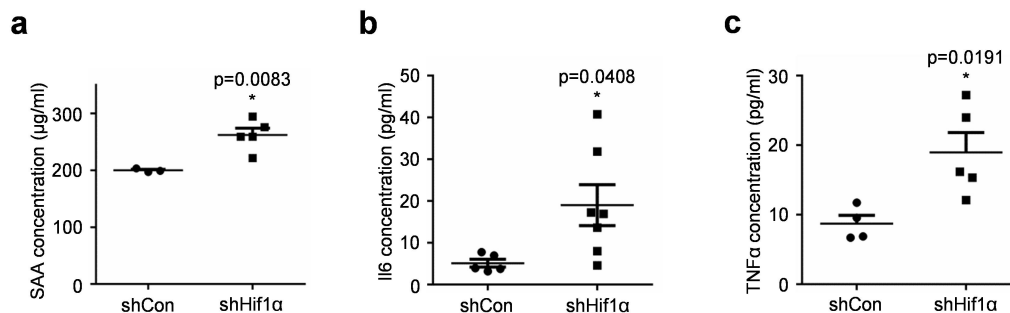
Figure 8.(a) SAA ELISA result shows increased SAA concentration in the serum of the shHif1α group; **(b-c)** Cytometric bead array experiments show elevated Il6 (b) and TNFα (c) concentration in the serum of the shHif1α group; The data are results of triplicate independent experiments and presented as mean±SEM; The *p* value is determined by unpaired *t*-test, n=5. This data has been already published in [49].

To further validate local immune cell infiltration, we performed immunohistochemistry staining of CD45 to examine the general immune cells distribution in the shCon group and the shHif1α group.

The positive stained cells could be observed both on the tumour border and the necrosis area (Figure 9a, left panel). However, there seemed no obvious differences of immune cells distribution in tumour border area between the shCon and the shHif1α (Figure 9a, middle panel). Interestingly, there were remarkably more cells infiltrated in the necrosis area of tumours from the shHif1α group (Figure 9a, right panel). Further positive cell quantification validated that the number of immune cells in the shHif1α group was 2.4 folds larger than that in the shCon group (Figure 9b, right panel, p=0.001).
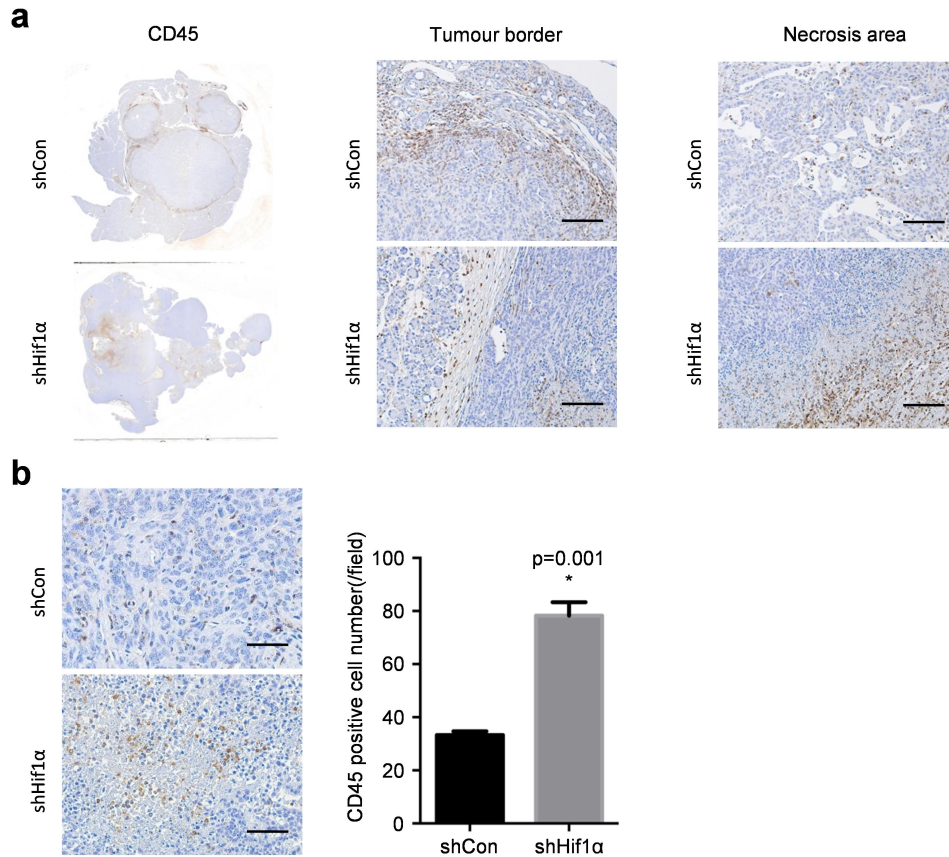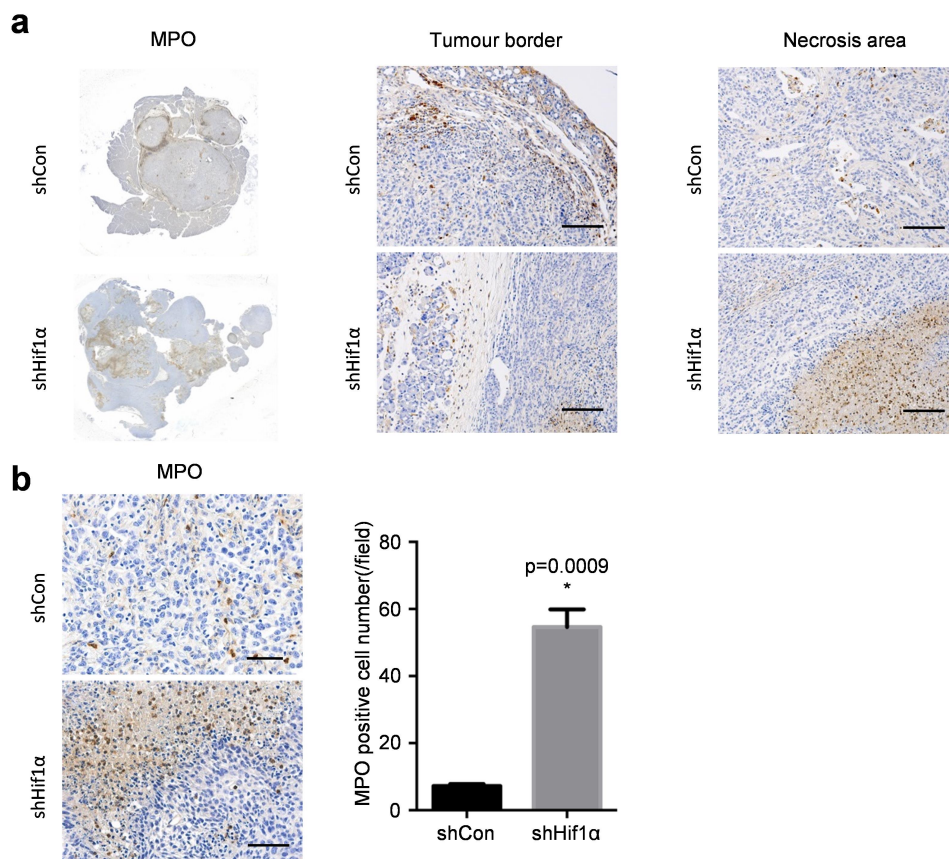
Figure 9. (a) IHC staining of CD45 shows observable immune cells both on tumour border and necrosis area, scale bar: 100 μm; **(b)** Representative pictures of CD45 and positive cells quantification demonstrate elevated immune cells infiltration in the necrosis area, scare bar: 200 μm, (n=5);The data are presented asmean±SEM; The *p* value is determined by unpaired *t*-test. This data has been already published in [49].

Next, we wanted to classify and locate these infiltrated immune cells.

When tissue damage occurs, neutrophil is the first responsible immune cell recruited to the inflammatory area [54]. Thus we evaluated neutrophil infiltration by performing myeloperoxidase (MPO) staining. The neutrophils were detectable both on tumour border and necrosis area (Figure 10a, left panel), and there were no significant differences of cell distribution in the

tumour border area between two groups (Figure 10a, middle panel). Interestingly, there were more MPO-positive cells in the necrosis area from the shHif1α group (Figure 10a, right panel). Positive cell quantification also proved that neutrophil infiltration in the shHif1α group was significantly 7.6 folds higher than that in the shCon group (Figure 10b, right panel, p=0.0009).

Figure 10. (a) IHC staining of MPO shows observable neutriphils both on tumour border and necrosis area, scale bar: 100 µm; **(b)** Representative pictures of MPO and positive cells quantification demonstrate elevated neutriphils infiltration in the necrosis area, scare bar: 200 µm, (n=5);The data are presented asmean±SEM; The *p* value is determined by unpaired *t*-test. This data has been already published in [49].

Apart from neutrophils, T cells are main force and regulator of adaptive immunity. They are also closely connected with PDAC progression, overall and disease-free survival time [55]. Thus we performed CD3 staining to mark T cell infiltration in two groups. T cells were mainly distributed in the solid rather than necrotic area of the tumour in two groups. No differences of T cell distribution were observed on the tumour border area (data not show). However, on contrary to neutrophils, there were significant less T cells infiltrated in the other solid tumour area (Figure 11 a-b, 33 vs 78 /field of view, p<0.0001). These result indicated that absence of Hif1α led to T cell extinction, suggesting a possible correlation between Hif1α and T cell function in PDAC.
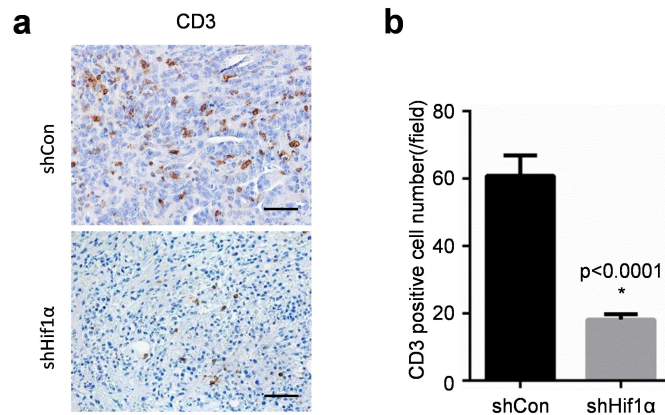
Figure 11. (a) IHC staining of CD3 shows decreased T cells in the tumour area, scale bar: 200 μm. **(b)** Positive stained cells quantification demonstrates obvious decrease of T cells in the tumour area (n=5); The data are presented asmean±SEM. The *p* value is determined by unpaired *t*-test. This data has been already published in [49].

A recent publication observed that loss of Hif1αmediated B cell infiltration [35], thus we also examined B cell infiltration in the shCon and shHif1α group by

performing B220 staining. In our study, the B cells were only observed on the border of the tumour and normal pancreas tissue, not in the necrosis or adjacent area (Figure 12a).In addition, positive cell quantification further verificated that there were no differences of B cell infiltration between the shCon group and shHif1α group(Figure 12b), suggesting B cell was not responsible for tumour growth promotion in our study.
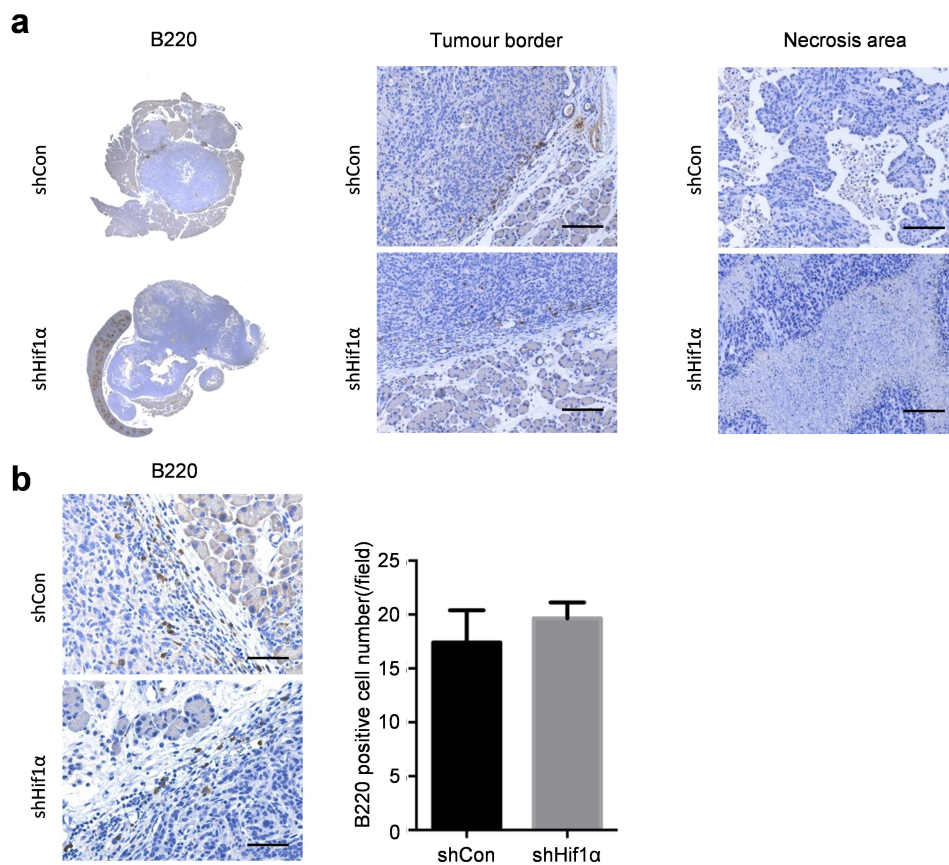
Figure 12. (a) IHC staining of B220 shows observable B cells only on tumour border, not in the necrosis area, scale bar: 100 μm; **(b)** Positive stained cells quantification shows no obvious differences of B cell infiltration between both groups, scale bar: 200 μm (n=5); The data are presented as mean±SEM; The *p* value is determined by unpaired *t*-test. This data has been already published in [49].

Apart from neutrophils, T cells and B cells, macrophages are the other major elements in the inflammatory microenvironment. Therefore, last we examined macrophage distribution by performing F4/80 immunohistochemistry staining. Similar to B cells, macrophages were only observable on the tumour border area, barely in the necrosis area (Figure 13a). Positive cell quantification showed that there were no differences of macrophages distribution in the tumour border area between two groups (Figure 13b)
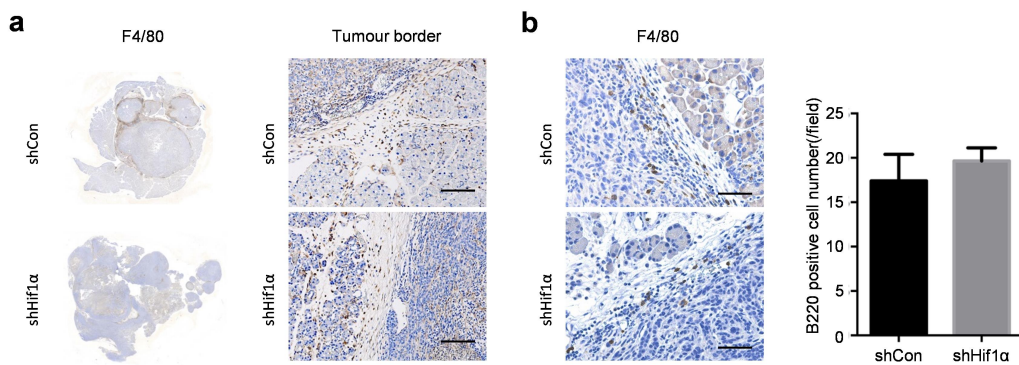

Figure 13. (a) IHC staining of F4/80 shows observable macrophages only on tumour border, not in the necrosis area, scale bar: 100 µm; **(b)** Positive stained cells quantification shows no obvious differences of macrophages infiltration on the tumour border between both groups, scale bar: 200 µm (n=5); The data are presented as mean±SEM; The p value is determined by unpaired t-test. This data has been already published in [49].

Taken together, our study proved that absence of Hif1α resulted in increased inflammation response, neutrophils infiltration and T cells extinction. The alteration if immune microenvironment might be correlated with elevated proliferation capacity in the shHif1α group.

The preliminary in vitro result revealed that Hif1α deficiency leads to invasion inhibition in our murine PDAC cells. Next, we wanted to examine the colonization/metastasis ability in vivo. Therefore, portal vein inoculation was performed to investigate distant organ metastasis.

As expected the shHif1α cells developed a significantly less hepatic metastasis than control cells (Figure 14a). The metastasis area of four liver lobes was 13.3 fold lower in the shHif1α group than that in the shControl group (Figure 14b, $p<0.0001$). Since the portal vein was inoculated with the same amount of tumour cells, the remarkable differences of liver metastasis might be an integrated result with other biological events.
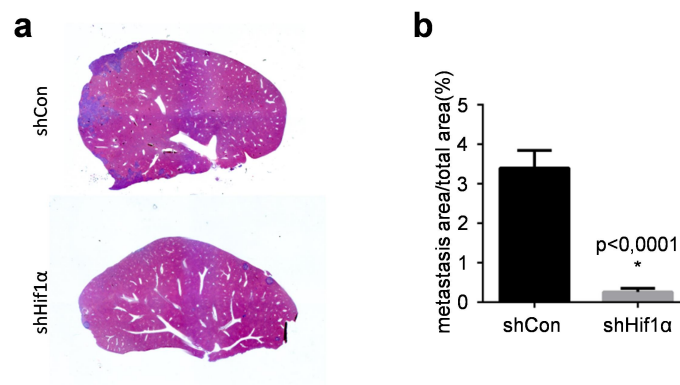

Figure 14. (a) Representative pictures of H&E staining shows less metastasis area in Hif1αdeletion group; **(b)** Necrotic area measurement confirms the metastasis reduction in Hif1αdeletion group (n=5); All data are present as mean±SEM and *p* value is determined by unpaired *t*-test. This data has been already published in [49].

To disseminate and colonise in the target organ, tumour cells need to overcome the loss of cell-cell interaction, enter circulation systems and survive in the anchorage-independent state. In consideration of the past result, we

speculated that Hif1α was crucial for cell survival in anchorage independent state.

The anoikis assay showed that less cell survived in the shHif1αgroup under anchorage-independent conditions (Figure15a, left panel). The viability of the shHif1α cells was significant lower than that of the shCon cells (Figure 15a, right panel, 16.94±0.60% vs 29.34±0.86%, p<0.0001). Hif1α deficient cells were more vulnerable to programmed cell death induced by stressed under anchorage independent conditions (Figure 15b, right panel, p=0.0093).
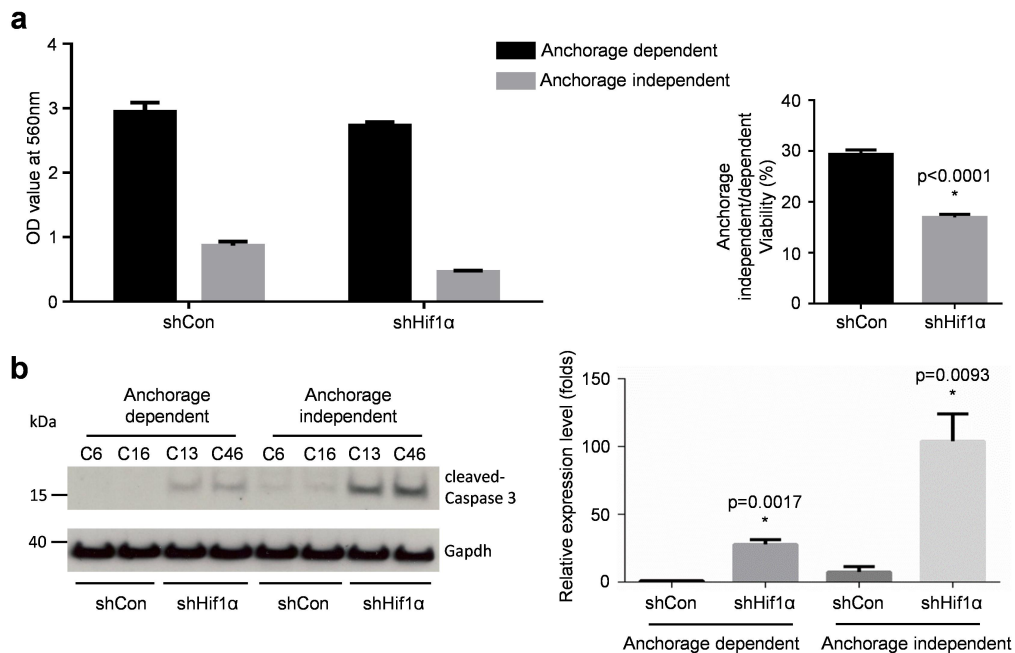
Figure 15. (a) Anoikis assay shows less cell survived under anchorage independent state in Hif1α deficiency group; **(b)** Western blot and quantification analysis shows upregulation of cleaved-Caspase 3 expression under anchorage independent state; All data are presented as aresult of three independent experiments, which are present as mean±SEM and *p* value is determined by unpaired *t*-test. This data has been already published in [49].

In spite of survival in anchorage-independent state, it is same crucial for PDAC cells to attach and colonize in new target organ. There have been evidence proved that PDAC cells produced and released some extracellular protein or exosome to "pre-educate" the target organ for better adherent and colonization [56, 57]. Thus next we examined influences of Hif1α depletion on extracellular matrix (ECM) protein with extracellular matrix and adhesion molecules array assays.

Interestingly, knock-down of Hif1α downregulated most part of the ECM and adhesion related protein (21 out of 88),only upregulate 6 correlated genes (Figure 16). Most genes from the Collagens gene family (Col1a1, Col4a1, Col4a2, Col6a1), Integrins gene family (Itga3,Itgb2, Itgb3), Laminin subunits gene family (Lamb2, Lamb3, Lamc1) and Matrix metalloproteinase gene family (MMP1a, MMP9, MMP11, MMP15) were downregulated 2.4 folds to 19 folds (Table 1). These data demonstrated that the disability of forming metastasis in Hif1α knock down group might due to aberrant ECM proteins and adhesion molecular expression, which failed to assist metastatic PDAC cells to settle down in the liver.
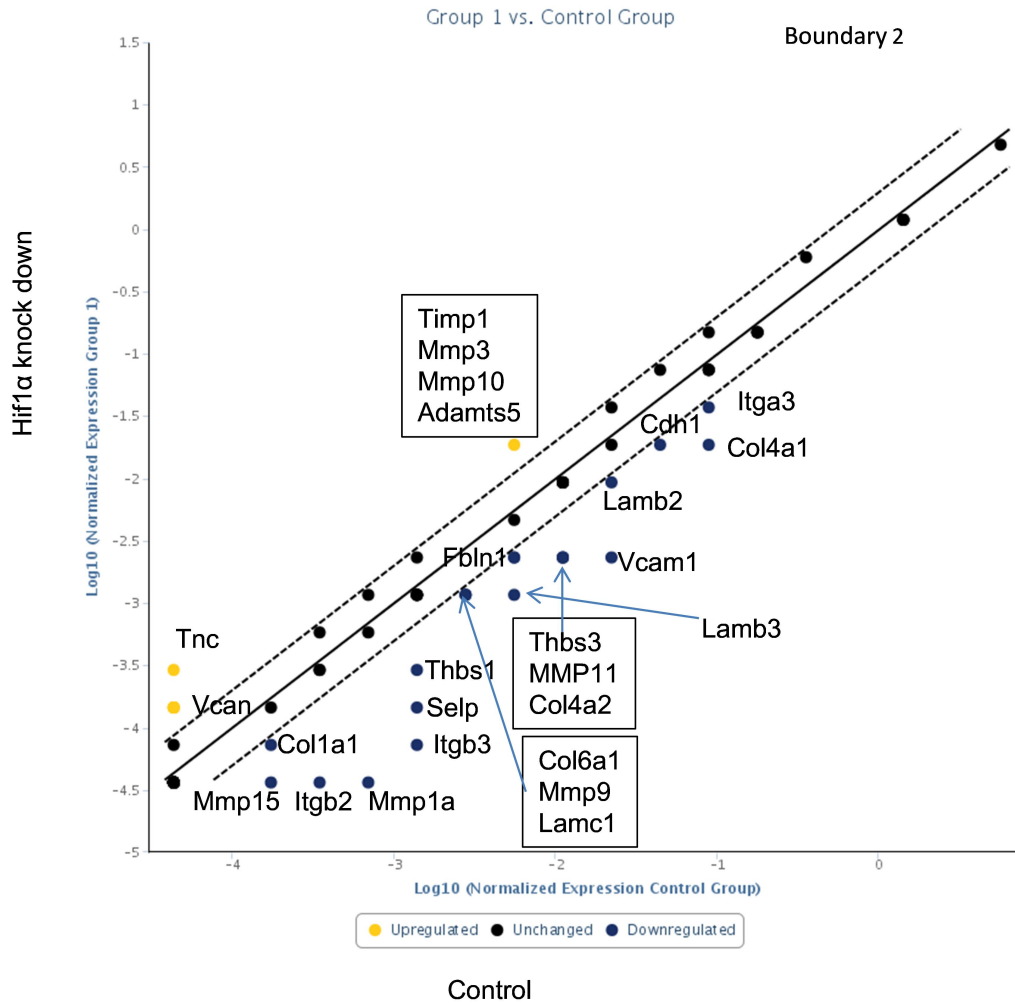
Figure 16. Scatter plot of ECM and adhesion moleculars array analysis between shCon group and shHif1α group.

Table 1. ECM and adhesion molecular genes expression

(shHif1α vs shCon)

Gene Symbol	Fold Regulation
Adamts5	3.3636
Mmp10	3.3636
Mmp3	3.3636

Timp1	3.3636
Tnc	6.7272
Vcan	3.3636
Cdh1	-2.3784
Col1a1	-2.3784
Col4a1	-4.7568
Col4a2	-4.7568
Col6a1	-2.3784
Fbln1	-2.3784
Itga3	-2.3784
Itgb2	-9.5137
Itgb3	-19.0273
Lamb2	-2.3784
Lamb3	-4.7568
Lamc1	-2.3784
Mmp11	-4.7568
Mmp15	-4.7568
Mmp1a	-19.0273
Mmp9	-2.3784
Ncam1	-2.3784
Selp	-9.5137
Thbs1	-4.7568
Thbs3	-4.7568

|	
Vcam1	-9.5137

Red colour: genes upregulated in the shHif1α group compare to the shCon group; Blue colour: genes downregulated in the shHif1α group compare to the shCon group.

5.0 DISCUSSION

Pancreatic cancer is one of the most devastating and highly metastatic cancer. Most of the patients suffered from distant organ metastasis at initial diagnosis [58]. Thus, it is extremely necessary to understand metastasis mechanism in pancreatic cancer.

Cancer metastasis is composed of sequential events, requiring multiple signallings and cascades involving in a complex process. Generally, it can be divided into four periods: (1) disrupt cell to cell interaction, acquire mobility and detach from the primary location; (2) penetrate and invade the surrounding extracellular matrix; (3) enter the circulatory system and survive under anoikis state; (4) disseminate, extravasate and colonize in favorable distant organ [59] (Figure 17).
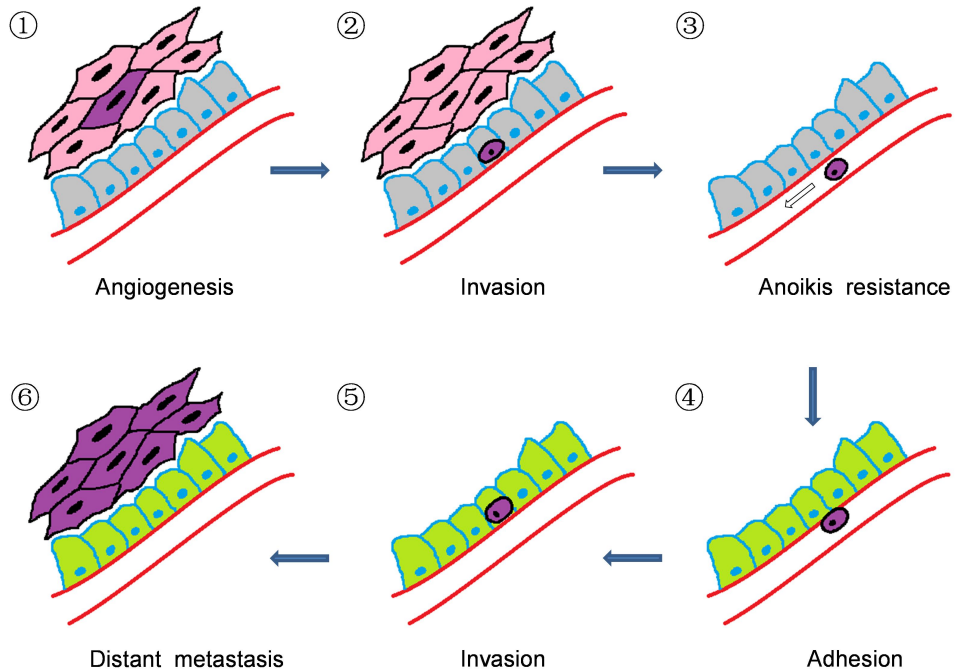
Figure 17. Sketch view of tumour metastasis. ⬟ : Primary tumour cells;

⬟ : Basement membrane cells in primary organ; ⬟ : Metastatic tumour

cells; ⬟ : Basement membrane cells in metastatic organ; ⫽ : Vessels.

Since hypoxia can be observed in the initiating stage of pancreatic carcinogenesis, as a sensor and master regulator of hypoxia, Hif1α is closely related to every step of pancreatic cancer metastasis. Indeed, our study observed that absence of Hif1α diminished pancreatic cancer metastasis in every aspect.

Wang and the co-workers reported that decreased expression of Hif1α impair cell invasion and suppress malignant phenotype in triple-negative breast cancer cells [60]. Our study also showed the presence of Hif1α contributes to the invasive character of murine PDAC cells in both normoxic and hypoxic conditions. These results demonstrate that Hif1α facilitate PDAC tumour cell motility.

As a hallmark of cancer, angiogenesis is important in assisting tumour growth and metastasis. The newly formed vessels relieve hypoxia pressure, provide tumour cells with necessary nutrients. VEGF, one of the most important proangiogenic factors in angiogenesis, is transcriptionally regulated by Hif1α [61].Consistent with previous data [62], our study observed a decreased Vegfa protein secretion in Hif1α knock-down cells.

A challenge for adherent tumour cells is to survive in anchorage-independent conditions after intravasating into the circulatory system. Due to lack of cell-cell interaction and adherence to extracellular matrix, it is very harsh for tumour cells to survive. The majority of epithelial cells undergo apoptosis while surviving cells acquire anoikis resistance.

In our study, Hif1α deletion led to significant reduction of cell viability under the anchorage-independent conditions, which verifies the pivotal role of Hif1α in mediating anoikis assistance.

Recently, it has been illustrated that the anoikis protective role of Hif1α may be related in regulating EMT process [17], EGFR signalling pathway [21] or integrin suppression [63]. In our study, the elevated cleaved-Caspase 3 expression in the Hif1α knock-down group indicated that apart from the above

mentioned signalling, apoptosis may also play vital roles in regulating anoikis resistance.

The last step of metastasis is to colonize the recipient organ. Zhao and the co-workers revealed that HIF1 contributed to converting cell metabolism from oxidative phosphorylation to glycolysis, therefore decreased intracellular ROS accumulation and benefited metastatic cell colonisation in the lung [64]. These data reflected that metabolic traits affected metastasis and colonization ability in tumour cells. Indeed, our results showed that when Hif1α is deleted from PDAC cells, the glucose uptake and intracellular glutamate are diminished by 50%, which revealed a general abbreviated metabolic pool in the Hif1α deleted tumour cells. The tough energy status will probably prevent the metastatic cells from surviving and colonising in the target organ. Indeed, there is less metastatic foci formed in our Hif1α knock-down group.

Except from survival in the target organ, it is also crucial for tumour cells to create feasible environment to attach and colonize. Some pivotal ECM proteins, such as Collagen Type VI Alpha 1 (Col6a1), Secreted Phosphoprotein 1 (Spp1) and Fibronectin 1 (Fn1) were reported to control metastasis switch in PDAC [65]. Thus, suitable microenvironment can be considered as determine point of metastasis. Our study found that knock down of Hif1α extensively downregulated ECM and adhesion associated genes, which explained the disability of hepatic metastasis in the shHif1α group.

Collectively, our results demonstrate an integral role of Hif1α in supporting cancer metastasis from enhancing tumour invasion, angiogenesis, anoikis resistance, and colonisation.

Since Hif1α is widely involved in cancer metastasis, it is important to develop inhibitors to target Hif1α or its downstream signalling pathways to impair tumour progression and cancer metastasis.

As introduced in the former section, there are two types of hypoxia inhibitors, which are TH-302 and PX-478. In particular, PX-478 is designed specifically targeting on Hif1α gene.

To date, PX-478 shows promising effect when applied in combination with gemcitabine on PDAC xenograft mouse model[39, 66]. Moreover, clinical trial declares a positive effect on preventing cancer progression in PX-478 alone application group [41], which may shed light on a new strategy to treat PDAC.

However, is the strategy targeting Hif1α as effective as we expected?

Though Whelan reported the absence of HIF1 inhibited tumour cell survival [67], our in vivo orthotopic injection mouse model revealed an unexpected result in the Hif1α knock-down group, which was that loss of Hif1α facilitates cell proliferation and necrosis in PDAC.

Since no proliferation differences were observed between control and Hif1α knock-down group in vitro, a possible explanation is the synergistic effect of other cells in the microenvironment. Due to fast expansion and disability of angiogenesis, Hif1α deletion group exhibited highly necrosis in tumour mass. It is well known necrotic cells induce inflammation, and immune cells are an

important component of the tumour microenvironment, it seems possible that immune cell infiltration might be responsible for facilitating Hif1α deletion cell proliferation.

Lee and the co-workers found out that Hif1α deficiency modulated B cell infiltration and accelerated PDAC initiation [35]. Thus we examined B cell infiltration between control and Hif1α knock-down group. Surprisingly, there was no obviously enhanced B cell infiltration. Instead, neutrophils infiltrated more in the Hif1α deletion group. Moreover, neutrophils-producing cytokines IL-6 and TNF-α were also elevated in mouse serum of Hif1α knock-down group, which suggesting that neutrophil infiltration might be responsible for promoting Hif1α deletion cell proliferation. The underlying mechanisms need further investigation.

Apart from aberrant neutrophils infiltration, we also observed that T cells were significantly suppressed in the Hif1α knock-down group, which highlighted a possibility of T cell extinction in response to tumour necrosis. Indeed, a recent publication found similar result in a mice-bearing-melanoma model as well as in human tumours. A recent report showed that tumour associated necrosis resulted in elevated potassium concentration in the extracellular microenvironment, which further suppressed T cell function by impairing activity of PP2A – a key downstream enzyme of Akt–mTOR signalling [68]. However, it is still unclear about the exact mechanism of T cell depletion in regulating tumour cell proliferation, which needs further investigation and exploration.

Collectively, we found in our study that the role of Hif1α in pancreatic tumorigenesis is context-dependent. Though deletion of Hif1α impairs distant organ metastasis, it results in increased tumour growth as well as pronounced necrosis in vivo. Our data hints that single application of Hif1α inhibitors should be considered cautiously, especially for the patients receiving palliative or adjuvant therapy. Besides, the application of Hif1α inhibitor in combination with immunotherapy should be tested in clinical setting.

6.0 SUMMARY

In this study, we investigated the role of Hif1α in PDAC in two major biological scenarios: tumour growth and remote colonisation. We observed that Hif1α deletion had no effect on cell proliferation in vitro, but promoted primary tumour growth in vivo. Further investigation proved that deletion of Hif1α rendered tumour cells more vulnerable to hypoxia-induced cell death, which triggered necrosis and subsequently promoted immune cell infiltration (especially neutrophils). The infiltrated immune cells are closely correlated with increased tumour growth in the Hif1α knock-down group. In addition, deletion of Hif1α impaired invasion capacity in vitro, also resulted in cell death under anchorage independent conditions, which further led to metastasis disability in vivo.

Therefore we answered the questions raised in the "Aim of the study" section as follows:

Question 1 (Q1): What is the effect of Hif1αdeletion on murine PDAC cells?

Conclusion 1 (C1): Deletion of Hif1α led to decreased glucose uptake, glutamine uptake, lactate secretion and Vegfa secretion. It had no effect on cell proliferation but impaired invasion ability.

Question 2(Q2): What is the in vivo function of Hif1α?

Conclusion 2(C2): Depletion of Hif1α in murine PDAC cells promoted primary tumour growth by recruiting immune cells (especially neutrophils) infiltration in vivo. Meanwhile it impaired tumour metastasis by inducing anchorage independent associated cell death.

Question 3(Q3): Is it practical to apply HIF1α inhibitors in clinical management?

Conclusion 3(C3): Since HIF1α plays a context-dependent role in pancreatic carcinogenesis, the application of HIF1α inhibitors should be carried out with caution. In treating primary pancreatic cancer, Hif1α should be applied in combination with other immune therapies. However, it might be a promising strategy to targeting circulating tumour cells.

7.0 ABBREVIATIONS

ATP	Adenosine triphosphate
ANG-1	Angiopoietin 1
ANG-2	Angiopoietin 2
BSA	Bovine serum albumin
Casp3	Caspase 3
CCL2	Chemokines 2
Col1a1	Collagen Type I Alpha 1
Col4a1	Collagen Type IV Alpha 1
Col4a2	Collagen Type IV Alpha 2
Col6a1	Collagen Type VI Alpha 1
Cre	Cre recombinase
DG6P	2-Deoxy-Glucose-6-Phosphate
ECM	Extracellular matrix
EGFR	Epidermal growth factor receptor
EMT	Epithelial-to-mesenchymal transition
FBS	Fetal bovine serum
Fn1	Fibronectin 1
GAPDH	Glyceraldehyde-3-phosphate dehydrogenase
GEM	Genetically engineered modified
GPX	Glutathione peroxides

Gls	Glutaminase
HIFs	Hypoxia-inducible factors
Hk2	Hexokinase-2
HRP	Horseradish peroxidase
IHC	Immunohistochemistry
Il6	Interleukin 6
Itga3	Integrin subunit alpha 3
Itgb2	Integrin subunit beta 2
Itgb3	Integrin subunit beta 3
KCl	Potassium chloride
KRAS	V-Ki-ras2 Kirsten rat sarcoma viral oncogene homolog
Lamb2	Laminin subunit beta 2
Lamb3	Laminin subunit beta 3
Lamc1	Laminin subunit gamma 1
LDHA	Lactate dehydrogenase
MAPK	Mitogen-activated protein kinase
MMP1	Matrix Metallopeptidase 1
MMP9	Matrix Metallopeptidase 9
MMP11	Matrix Metallopeptidase 11
MMP15	Matrix Metallopeptidase 15
mTOR	mechanistic target of rapamycin
MTT	3-(4,5-dimethylthiazole-2-yl)2,5-diphenyltetrazolium bromide

MPO	Myeloperoxidase
PanIN	Pancreatic intraepithelial neoplasia
PARP1	Poly (ADP-ribose) polymerase 1
PBS	Phosphate buffered saline
PDAC	Pancreatic ductal adenocarcinoma
PDGF	Platelet-derived growth factor
PDH	pyruvate dehydrogenase
PKM2	pyruvate kinase M2
ROS	Reactive oxygen species
SAA	serum amyloid A
SDS	Laurylsulfate
shCon	Scramble plasmid
shHif1α	Hif1α knock-down plasmid
Spp1	Secreted phosphoprotein 1
TNFα	Tumour necrosis factor α
TSC	Tuberous sclerosis
VEGF	Vascular endothelial growth factor
WB	Western blot

8.0 REFERENCES

[1] Gnaiger E., Steinlechner-Maran R., Mendez G., Eberl T. & Margreiter R. (1995). Control of mitochondrial and cellular respiration by oxygen. *J Bioenerg Biomembr*, 27(6), 583-96.

[2] Pettersen E. O., Ebbesen P., Gieling R. G., Williams K. J., Dubois L., Lambin P., Ward C., Meehan J., Kunkler I. H., Langdon S. P., Ree A. H., Flatmark K., Lyng H., Calzada M. J., Peso L. D., Landazuri M. O., Gorlach A., Flamm H., Kieninger J., Urban G., Weltin A., Singleton D. C., Haider S., Buffa F. M., Harris A. L., Scozzafava A., Supuran C. T., Moser I., Jobst G., Busk M., Toustrup K., Overgaard J., Alsner J., Pouyssegur J., Chiche J., Mazure N., Marchiq I., Parks S., Ahmed A., Ashcroft M., Pastorekova S., Cao Y., Rouschop K. M., Wouters B. G., Koritzinsky M., Mujcic H. & Cojocari D. (2015). Targeting tumour hypoxia to prevent cancer metastasis. From biology, biosensing and technology to drug development: the METOXIA consortium. *J Enzyme Inhib Med Chem*, 30(5), 689-721.

[3] Bertout J. A., Patel S. A. & Simon M. C. (2008). The impact of O2 availability on human cancer. *Nat Rev Cancer*, 8(12), 967-75.

[4] Imtiyaz H. Z. & Simon M. C. (2010). Hypoxia-inducible factors as essential regulators of inflammation. *Curr Top Microbiol Immunol*, 345(105-20.

[5] Zwaans B. M. & Lombard D. B. (2014). Interplay between sirtuins, MYC and hypoxia-inducible factor in cancer-associated metabolic reprogramming. *Dis Model Mech*, 7(9), 1023-32.

[6] Harris A. L. (2002). Hypoxia--a key regulatory factor in tumour growth. *Nat Rev Cancer*, 2(1), 38-47.

[7] Hanahan D. & Weinberg R. A. (2011). Hallmarks of cancer: the next generation. *Cell*, 144(5), 646-74.

[8] Semenza G. L. (2002). Involvement of hypoxia-inducible factor 1 in human cancer. *Intern Med*, 41(2), 79-83.

[9] Lee J. W., Bae S. H., Jeong J. W., Kim S. H. & Kim K. W. (2004). Hypoxia-inducible factor (HIF-1)alpha: its protein stability and biological functions. *Exp Mol Med*, 36(1), 1-12.

[10] Risau W. (1997). Mechanisms of angiogenesis. *Nature*, 386(6626), 671-4.

[11] Zimna A. & Kurpisz M. (2015). Hypoxia-Inducible Factor-1 in Physiological and Pathophysiological Angiogenesis: Applications and Therapies. *Biomed Res Int*, 2015(549412.

[12] Rankin E. B. & Giaccia A. J. (2008). The role of hypoxia-inducible factors in tumorigenesis. *Cell Death Differ*, 15(4), 678-85.

[13] Gastl G., Hermann T., Steurer M., Zmija J., Gunsilius E., Unger C. & Kraft A. (1997). Angiogenesis as a target for tumor treatment. *Oncology*, 54(3), 177-84.

[14] Semenza G. L. (2012). Molecular mechanisms mediating metastasis of hypoxic breast cancer cells. *Trends Mol Med*, 18(9), 534-43.

[15] Michel G., Tonon T., Scornet D., Cock J. M. & Kloareg B. (2010). The cell wall polysaccharide metabolism of the brown alga Ectocarpus siliculosus. Insights into the evolution of extracellular matrix polysaccharides in Eukaryotes. *New Phytol*, 188(1), 82-97.

[16] Chiarugi P. & Giannoni E. (2008). Anoikis: a necessary death program for anchorage-dependent cells. *Biochem Pharmacol*, 76(11), 1352-64.

[17] Paoli P., Giannoni E. & Chiarugi P. (2013). Anoikis molecular pathways and its role in cancer progression. *Biochim Biophys Acta*, 1833(12), 3481-98.

[18] Wu Y. & Zhou B. P. (2010). Snail: More than EMT. *Cell Adh Migr*, 4(2), 199-203.

[19] Imai T., Horiuchi A., Wang C., Oka K., Ohira S., Nikaido T. & Konishi I. (2003). Hypoxia attenuates the expression of E-cadherin via up-regulation of SNAIL in ovarian carcinoma cells. *Am J Pathol*, 163(4), 1437-47.

[20] Wheaton W. W. & Chandel N. S. (2011). Hypoxia. 2. Hypoxia regulates cellular metabolism. *Am J Physiol Cell Physiol*, 300(3), C385-93.

[21] Whelan K. A., Caldwell S. A., Shahriari K. S., Jackson S. R., Franchetti L. D., Johannes G. J. & Reginato M. J. (2010). Hypoxia suppression of Bim and Bmf blocks anoikis and luminal clearing during mammary morphogenesis. *Mol Biol Cell*, 21(22), 3829-37.

[22] Zhang H., Bosch-Marce M., Shimoda L. A., Tan Y. S., Baek J. H., Wesley J. B., Gonzalez F. J. & Semenza G. L. (2008). Mitochondrial autophagy is an HIF-1-dependent adaptive metabolic response to hypoxia. *J Biol Chem*, 283(16), 10892-903.

[23] Semenza G. L. (2013). HIF-1 mediates metabolic responses to intratumoral hypoxia and oncogenic mutations. *J Clin Invest*, 123(9), 3664-71.

[24] Talks K. L., Turley H., Gatter K. C., Maxwell P. H., Pugh C. W., Ratcliffe P. J. & Harris A. L. (2000). The expression and distribution of the hypoxia-inducible factors HIF-1alpha and HIF-2alpha in normal human tissues, cancers, and tumor-associated macrophages. *Am J Pathol*, 157(2), 411-21.

[25] Luo W., Hu H Fau - Chang R., Chang R Fau - Zhong J., Zhong J Fau - Knabel M., Knabel M Fau - O'Meally R., O'Meally R Fau - Cole R. N., Cole Rn Fau - Pandey A., Pandey A Fau - Semenza G. L. & Semenza G. L. Pyruvate kinase M2 is a PHD3-stimulated coactivator for hypoxia-inducible factor 1. 1097-4172 (Electronic)),

[26] Inman K. S., Francis A. A. & Murray N. R. (2014). Complex role for the immune system in initiation and progression of pancreatic cancer. *World J Gastroenterol*, 20(32), 11160-81.

[27] Matzinger P. (2002). The danger model: a renewed sense of self. *Science*, 296(5566), 301-5.

[28] Kaufmann S. H. (1999). Cell-mediated immunity: dealing a direct blow to pathogens. *Curr Biol*, 9(3), R97-9.

[29] Grivennikov S. I., Greten F. R. & Karin M. (2010). Immunity, inflammation, and cancer. *Cell*, 140(6), 883-99.

[30] Clark C. E., Hingorani S. R., Mick R., Combs C., Tuveson D. A. & Vonderheide R. H. (2007). Dynamics of the immune reaction to pancreatic cancer from inception to invasion. *Cancer Res*, 67(19), 9518-27.

[31] Taylor C. T. (2008). Interdependent roles for hypoxia inducible factor and nuclear factor-kappaB in hypoxic inflammation. *J Physiol*, 586(17), 4055-9.

[32] Triner D. & Shah Y. M. (2016). Hypoxia-inducible factors: a central link between inflammation and cancer. *J Clin Invest*, 126(10), 3689-3698.

[33] Erickson L. A., Highsmith W. E., Jr., Fei P. & Zhang J. (2015). Targeting the hypoxia pathway to treat pancreatic cancer. *Drug Des Devel Ther*, 9(2029-31.

[34] Li N., Li Y., Li Z., Huang C., Yang Y., Lang M., Cao J., Jiang W., Xu Y., Dong J. & Ren H. (2016). Hypoxia Inducible Factor 1 (HIF-1) Recruits Macrophage to Activate Pancreatic Stellate Cells in Pancreatic Ductal Adenocarcinoma. *Int J Mol Sci*, 17(6),

[35] Lee K. E., Spata M., Bayne L. J., Buza E. L., Durham A. C., Allman D., Vonderheide R. H. & Simon M. C. (2016). Hif1a Deletion Reveals Pro-Neoplastic Function of B Cells in Pancreatic Neoplasia. *Cancer Discov*, 6(3), 256-69.

[36] Bailey K. M., Cornnell H. H., Ibrahim-Hashim A., Wojtkowiak J. W., Hart C. P., Zhang X., Leos R., Martinez G. V., Baker A. F. & Gillies R. J. (2014). Evaluation of the "steal" phenomenon on the efficacy of hypoxia activated prodrug TH-302 in pancreatic cancer. *PLoS One*, 9(12), e113586.

[37] Borad M. J., Reddy S. G., Bahary N., Uronis H. E., Sigal D., Cohn A. L., Schelman W. R., Stephenson J., Jr., Chiorean E. G., Rosen P. J., Ulrich B., Dragovich T., Del Prete S. A., Rarick M., Eng C., Kroll S. & Ryan D. P. (2015). Randomized Phase II Trial of Gemcitabine Plus TH-302 Versus Gemcitabine in Patients With Advanced Pancreatic Cancer. *J Clin Oncol*, 33(13), 1475-81.

[38] Koh M. Y., Spivak-Kroizman T., Venturini S., Welsh S., Williams R. R., Kirkpatrick D. L. & Powis G. (2008). Molecular mechanisms for the activity of PX-478, an antitumor inhibitor of the hypoxia-inducible factor-1alpha. *Mol Cancer Ther*, 7(1), 90-100.

[39] Zhao T., Ren H., Jia L., Chen J., Xin W., Yan F., Li J., Wang X., Gao S., Qian D., Huang C. & Hao J. (2015). Inhibition of HIF-1alpha by PX-478 enhances the anti-tumor effect of gemcitabine by inducing immunogenic cell death in pancreatic ductal adenocarcinoma. *Oncotarget*, 6(4), 2250-62.

[40] Lang M., Wang X., Wang H., Dong J., Lan C., Hao J., Huang C., Li X., Yu M., Yang Y., Yang S. & Ren H. (2016). Arsenic trioxide plus PX-478 achieves effective treatment in pancreatic ductal adenocarcinoma. *Cancer Lett*, 378(2), 87-96.

[41] Tibes R., Falchook G. S., Von Hoff D. D., Weiss G. J., Iyengar T., Kurzrock R., Pestano L., Lowe A. M. & Herbst R. S. (2010). Results from a phase I, dose-escalation study of PX-478, an orally available inhibitor of HIF-1α. *J Clin Oncol*, 28(abstr 3076.

[42] Kong B., Cheng T., Wu W., Regel I., Raulefs S., Friess H., Erkan M., Esposito I., Kleeff J. & Michalski C. W. (2015). Hypoxia-induced endoplasmic reticulum stress characterizes a necrotic phenotype of pancreatic cancer. *Oncotarget*, 6(31), 32154-60.

[43] Koong A. C., Mehta V. K., Le Q. T., Fisher G. A., Terris D. J., Brown J. M., Bastidas A. J. & Vierra M. (2000). Pancreatic tumors show high levels of hypoxia. *Int J Radiat Oncol Biol Phys*, 48(4), 919-22.

[44] Semenza G. L. (1999). Regulation of mammalian O2 homeostasis by hypoxia-inducible factor 1. *Annu Rev Cell Dev Biol*, 15(551-78.

[45] Shibaji T., Nagao M., Ikeda N., Kanehiro H., Hisanaga M., Ko S., Fukumoto A. & Nakajima Y. (2003). Prognostic significance of HIF-1 alpha overexpression in human pancreatic cancer. *Anticancer Res*, 23(6C), 4721-7.

[46] Zhong H., Chiles K., Feldser D., Laughner E., Hanrahan C., Georgescu M. M., Simons J. W. & Semenza G. L. (2000). Modulation of hypoxia-inducible factor 1alpha expression by the epidermal growth factor/phosphatidylinositol 3-kinase/PTEN/AKT/FRAP pathway in human prostate cancer cells: implications for tumor angiogenesis and therapeutics. *Cancer Res*, 60(6), 1541-5.

[47] Yamamoto N., Ueda M., Sato T., Kawasaki K., Sawada K., Kawabata K. & Ashida H. (2011). Measurement of glucose uptake in cultured cells. *Curr Protoc Pharmacol*, Chapter 12(Unit 12 14 1-22.

[48] Kong B., Wu W., Cheng T., Schlitter A. M., Qian C., Bruns P., Jian Z., Jager C., Regel I., Raulefs S., Behler N., Irmler M., Beckers J., Friess H., Erkan M., Siveke J. T., Tannapfel A., Hahn S. A., Theis F. J., Esposito I., Kleeff J. & Michalski C. W. (2016). A subset of metastatic pancreatic ductal adenocarcinomas depends quantitatively on oncogenic Kras/Mek/Erk-induced hyperactive mTOR signalling. *Gut*, 65(4), 647-57.

[49] Cheng T., Jian Z., Li K., Raulefs S., Regel I., Shen S., Zou X., Ruland J., Ceyhan G. O., Friess H., Michalski C. W., Kleeff J. & Kong B. (2016). In vivo functional dissection of a

context-dependent role for Hif1alpha in pancreatic tumorigenesis. *Oncogenesis*, 5(12), e278.

[50] Goda N., Dozier S. J. & Johnson R. S. (2003). HIF-1 in cell cycle regulation, apoptosis, and tumor progression. *Antioxid Redox Signal*, 5(4), 467-73.

[51] Forsythe J. A., Jiang B. H., Iyer N. V., Agani F., Leung S. W., Koos R. D. & Semenza G. L. (1996). Activation of vascular endothelial growth factor gene transcription by hypoxia-inducible factor 1. *Mol Cell Biol*, 16(9), 4604-13.

[52] Rock K. L. & Kono H. (2008). The inflammatory response to cell death. *Annu Rev Pathol*, 3(99-126.

[53] Mantovani A., Allavena P., Sica A. & Balkwill F. (2008). Cancer-related inflammation. *Nature*, 454(7203), 436-44.

[54] Powell D. R. & Huttenlocher A. (2016). Neutrophils in the Tumor Microenvironment. *Trends Immunol*, 37(1), 41-52.

[55] Bazhin A. V., Shevchenko I., Umansky V., Werner J. & Karakhanova S. (2014). Two immune faces of pancreatic adenocarcinoma: possible implication for immunotherapy. *Cancer Immunol Immunother*, 63(1), 59-65.

[56] Costa-Silva B., Aiello N. M., Ocean A. J., Singh S., Zhang H., Thakur B. K., Becker A., Hoshino A., Mark M. T., Molina H., Xiang J., Zhang T., Theilen T. M., Garcia-Santos G., Williams C., Ararso Y., Huang Y., Rodrigues G., Shen T. L., Labori K. J., Lothe I. M., Kure E. H., Hernandez J., Doussot A., Ebbesen S. H., Grandgenett P. M., Hollingsworth M. A., Jain M., Mallya K., Batra S. K., Jarnagin W. R., Schwartz R. E., Matei I., Peinado H., Stanger B. Z., Bromberg J. & Lyden D. (2015). Pancreatic cancer exosomes initiate pre-metastatic niche formation in the liver. *Nat Cell Biol*, 17(6), 816-26.

[57] Paron I., Berchtold S., Voros J., Shamarla M., Erkan M., Hofler H. & Esposito I. (2011). Tenascin-C enhances pancreatic cancer cell growth and motility and affects cell adhesion through activation of the integrin pathway. *PLoS One*, 6(6), e21684.

[58] Siegel R. L., Miller K. D. & Jemal A. (2015). Cancer statistics, 2015. *CA Cancer J Clin*, 65(1), 5-29.

[59] Valastyan S. & Weinberg R. A. (2011). Tumor metastasis: molecular insights and evolving paradigms. *Cell*, 147(2), 275-92.

[60] Wang F., Chang M., Shi Y., Jiang L., Zhao J., Hai L., Sharen G. & Du H. (2014). Down-regulation of hypoxia-inducible factor-1 suppresses malignant biological behavior of triple-negative breast cancer cells. *Int J Clin Exp Med*, 7(11), 3933-40.

[61] Pages G. & Pouyssegur J. (2005). Transcriptional regulation of the Vascular Endothelial Growth Factor gene--a concert of activating factors. *Cardiovasc Res*, 65(3), 564-73.

[62] Krock B. L., Skuli N. & Simon M. C. (2011). Hypoxia-induced angiogenesis: good and evil. *Genes Cancer*, 2(12), 1117-33.

[63] Rohwer N., Welzel M., Daskalow K., Pfander D., Wiedenmann B., Detjen K. & Cramer T. (2008). Hypoxia-inducible factor 1alpha mediates anoikis resistance via suppression of alpha5 integrin. *Cancer Res*, 68(24), 10113-20.

[64] Zhao T., Zhu Y., Morinibu A., Kobayashi M., Shinomiya K., Itasaka S., Yoshimura M., Guo G., Hiraoka M. & Harada H. (2014). HIF-1-mediated metabolic reprogramming reduces ROS levels and facilitates the metastatic colonization of cancers in lungs. *Sci Rep*, 4(3793.

[65] Whittle M. C., Izeradjene K., Rani P. G., Feng L., Carlson M. A., DelGiorno K. E., Wood L. D., Goggins M., Hruban R. H., Chang A. E., Calses P., Thorsen S. M. & Hingorani S. R. (2015). RUNX3 Controls a Metastatic Switch in Pancreatic Ductal Adenocarcinoma. *Cell*, 161(6), 1345-60.

[66] Sun J. D., Liu Q., Ahluwalia D., Li W., Meng F., Wang Y., Bhupathi D., Ruprell A. S. & Hart C. P. (2015). Efficacy and safety of the hypoxia-activated prodrug TH-302 in combination with gemcitabine and nab-paclitaxel in human tumor xenograft models of pancreatic cancer. *Cancer Biol Ther*, 16(3), 438-49.

[67] Whelan K. A., Schwab L. P., Karakashev S. V., Franchetti L., Johannes G. J., Seagroves T. N. & Reginato M. J. (2013). The oncogene HER2/neu (ERBB2) requires the hypoxia-inducible factor HIF-1 for mammary tumor growth and anoikis resistance. *J Biol Chem*, 288(22), 15865-77.

[68] Eil R., Vodnala S. K., Clever D., Klebanoff C. A., Sukumar M., Pan J. H., Palmer D. C., Gros A., Yamamoto T. N., Patel S. J., Guittard G. C., Yu Z., Carbonaro V., Okkenhaug K., Schrump D. S., Linehan W. M., Roychoudhuri R. & Restifo N. P. (2016). Ionic immune suppression within the tumour microenvironment limits T cell effector function. *Nature*, 537(7621), 539-543.

9.0 CURRICULUM VITAE

Familienname: Cheng

Vorname: Tao

Geburtsdatum: 14.07.1986

Geschlecht: männlich

Familienstatus: Ledig

Nationalität: Chinese

Adresse: Plettstr. 39, c/o Shi , 81735 München

Tel: 015161008076

Email: chengtao860714@hotmail.com

Ausbildung und beruflicher Werdegang:

12/2011-   Stipendiat, Anfertigung der medizinischen Doktorarbeit,

                  Technische Universität München

09/2009-06/2011   Master in Medizin, Southeast University, China

09/2004-06/2009   Bachelor in Medizin, Southeast University, China

Publikationen:

Kong B, Wu W, **Cheng T**, Schlitter AM, Qian C, Bruns P, Jian Z, et al. A subset of metastatic pancreatic ductal adenocarcinomas depends quantitatively on oncogenic Kras/Mek/Erk-induced hyperactive mTOR signalling. Gut. 2016 Apr;65(4):647-657

Kong B, **Cheng T**, Qian C, et al. Pancreas-specific activation of mTOR and loss of p53 induce tumors reminiscent of acinar cell carcinoma. Mol Cancer. 2015 Dec 18;14:212.

Kong B, **Cheng T**, Wu W, et al. Hypoxia-induced endoplasmic reticulum stress characterizes a necrotic phenotype of pancreatic cancer. Oncotarget. 2015 Oct 13;6(31):32154-32160.

Berchtold S, Grünwald B, Krüger A, Reithmeier A, Hähl T, **Cheng T**, et al. Collagen type V promotes the malignant phenotype of pancreatic ductal adenocarcinoma. Cancer Lett. 2015 Jan 28;356(2 Pt B):721-732

10.0 ACKNOWLEDGEMENTS